Adaptive Time Domain Equalizer (TEQ) for VDSL System

Pei-Ju Chung

Advisor: Dr. Yuan-Pei Lin
Department of Electrical and Control Engineering
National Chiao Tung University

August 2, 2005

Abstract

There has been great interest in DMT systems (Discrete Multitone) for high-speed transmission. The time domain equalizer (TEQ) plays an important role in such an application. The VDSL (Very-high-bit-rate Digital Subscriber Line)is an example of DMT systems. In this thesis, two adaptive TEQ design methods will be proposed. The proposed methods utilize training symbols in the initialization stage. We use an adaptive approach to train TEQ by exploiting the symbols in frequency domain. The simulation results will be given to illustrate the proposed TEQ methods can achieve good bit rates with only a small number of training symbols (iterations).

Contents

List of Figures

Chapter 1

Introduction

The DFT based DMT (discrete multitone) transceiver has found important application in DSL (digital subscriber loop). The transmitter and receiver perform respectively M-point IDFT and DFT computation, where M is the number of tones or number of subchannels. At the transmitter side, each block is padded with a cyclic prefix of length L. If L is no smaller than the order of the channel, then inter-block-interference (IBI) can be removed easily by discarding the prefix at the receiver. As a result, an FIR channel is converted into M frequency non-selective parallel subchannels. The subchannel gains are the M-point DFT of the channel impulse response. When the channel is longer or much longer than L, which is usually the case in DSL applications, a time domain equalizer (TEQ) is usually inserted at the receiver to shorten the channel impulse response so that the equivalent channel has most of the energy concentrated in a window of $L+1$ samples. The samples outside the window will lead to IBI and thus affects transmission bit rates. The time domain equalizers play an important role in the application of DMT to DSL.

There have been extensive researches of TEQ designs for DMT systems, such as bitrate maximizing TEQ[5][6], which uses subchannel SNR defined at the FEQ output by exploiting the dependance of the FEQs on the TEQ coefficients. Maximum geometric signal-to-noise ratio (MGSNR)[7][8][9], which maximizes the geometric mean of the subchannel SNRs in order to maximize the bit rate. In the per-tone equalization method[3] interchanges the TEQ and the DFT. As a result,

this TEQ design method could be considered as "frequency domain" equalizer. Maximum bit rate method (MBR)[4], which separates channel impulse response into two portions, signal and interference. The minimum mean square error (MMSE) method[10] shortens the channel impulse response to a target impulse response by minimizing the mean square error between the equivalent channel and the target impulse response. The method, Minimum delay spread (MDS)[11], minimizes the square of the delay spread of the effective channel.

Maximum shortening SNR (MSSNR)[15]. This proposed method is designed only based on the effective channel. It tries to maximize the desired window and minimize the walls of the effective channel. Multicarrier equalization by restoration of redundancy (MERRY)[12]; the TEQ design exploits the character of CP redundancy. Another TEQ design, Sum-squared auto-correlation minimization (SAM)[13], utilizes the autocorrelation of the effective channel. A frequency-domain SIR maximizing TEQ[16]; this is a semi-blind TEQ design method which maximizes signal-to-interference ratio (SIR) in frequency domain for VDSL systems. Those methods utilize many ways of designing equalizers and the last four designs will be described in detail in the thesis.

In this thesis, we propose two TEQ design methods which utilize training symbols in the initialization stage for VDSL system. We use an adaptive approach to train TEQ by exploiting the symbols in frequency domain. In the VDSL system frequency division duplex is used to separate upstream and downstream signals. In downstream or upstream application, there are only around half of the tones used and other unused tones are referred to as the null tones in this thesis. In VDSL training symbols, around half of the used tones are pilots and the other half carry message. We will exploit these properties of the training symbols to design TEQ. The proposed TEQ design methods are computed directly using an average of the received VDSL symbols without channel estimation. An estimate of the channel impulse response is more complex for VDSL system as not all the tone are used and the frequency response of the channel is available only on the tones used. Furthermore, not having to estimate the channel will also save training time. Besides, the objective function is formulated in frequency domain; the

optimization implicity takes into account equivalent channel's frequency response. The frequency response of the equivalent channel critically affects subchannel SNR and bit rate. One of the proposed TEQ is NM-TEQ (Null tone Minimizing TEQ) method which minimizes the null tone energy and the other proposed TEQ is PMNM-TEQ (Pilot tone Maximizing and Null tone Minimizing) method which maximizes the pilot tone energy and minimizes the null tone energy. They will be introduced in details in chapter 4. The simulation results will be given to illustrate the proposed TEQ methods can achieve good bit rates with only a small number of training symbols (iterations).

Outline

The thesis is organized as follows. In chapter 2, we give a survey of some existing TEQ design methods, including the method of Maximum shortening SNR[15], the MERRY algorithm[12], the SAM algorithm[13] and the blind equalization method in [14]. In chapter 3, we introduce the VDSL system and properties of VDSL initialization that will be useful for TEQ design. In chapter 4, we present the proposed TEQ design methods. Numerical simulations are shown in chapter 5, and a conclusion is given in chapter 6.

1.1 Notations

1. Bold face upper case letters represent matrices. Bold face lower case letters represent matrices. $\mathbf{A}^\top$ denotes transpose of $\mathbf{A}$, and $\mathbf{A}^\dagger$ denotes conjugate transpose of $\mathbf{A}$.

2. $\|\mathbf{x}\|$ denotes 2-norm of vector $\mathbf{x}$

3. The function $E[y]$ denotes the average value or expect value of y.

4. $eig(\mathbf{A})$ is the operation of finding eigenvalues of $\mathbf{A}$.

5. $*$ denotes the linear convolution operator.

6. $\star$ represents the complex conjugate operator.

Chapter 2

Existing TEQ design methods

In this chapter, we will give a survey of some existing TEQ design methods. In particular, we will introduce the method of Maximum shortening SNR[15], the MERRY algorithm[12], the SAM algorithm[13] and the blind equalization method in [14].

They are the Blind channel shortening of [12], the Blind equalization of multicarrier system[14], and Maximum shortening SNR from [15].

2.1   Maximun shortening SNR (MSSNR)

The MSSNR[15] technique attempts to minimize the energy outside the window which is composed of consecutive samples of length $L+1$ of the effective channel $\mathbf{c} = \mathbf{h} * \mathbf{t}$ (called the 'wall'), where L is the length of CP, and forcing as much of
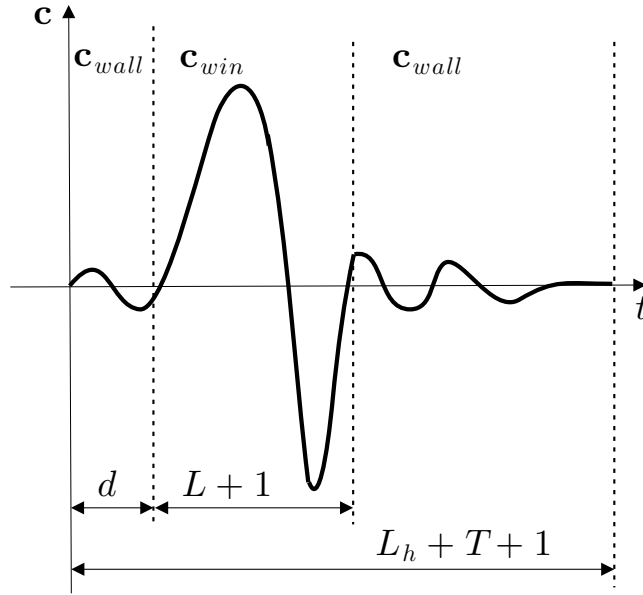
Figure 2.1: The "window" and "walls" of the effective channel

the the energy of the effective channel to lie in the desired window.

$$
\begin{aligned}
\mathbf{c} &= \begin{pmatrix} c(0) \\ c(1) \\ \vdots \\ c(L_h) \\ c(L_h+1) \\ \vdots \\ c(L_h+T-1) \end{pmatrix} \\
&= \begin{pmatrix} h(0) & 0 & \cdots & \cdots & 0 \\ h(1) & h(0) & \ddots & & \vdots \\ \vdots & \ddots & & & \vdots \\ h(L_h-1) & h(L_h-2) & \cdots & h(L_h-T+1) & h(L_h-T) \\ 0 & h(L_h-1) & \cdots & & h(L_h-T+1) \\ \vdots & \ddots & & & \vdots \\ 0 & \cdots & & 0 & h(L_h-1) \end{pmatrix} \begin{pmatrix} t(0) \\ t(1) \\ \vdots \\ t(T-1) \end{pmatrix} \\
&= \mathbf{H\,t} && (2.1)
\end{aligned}
$$

11

where L_h is the length of the impulse response of the physical channel, and T is the length of TEQ.

$$
\begin{aligned}
\mathbf{c}_{win} &= \begin{pmatrix} c(d) \\ c(d+1) \\ \vdots \\ c(d+L) \end{pmatrix} \\
&= \begin{pmatrix} h(d) & h(d-1) & \cdots & h(d-T+1) \\ h(d+1) & h(d) & \cdots & h(d-T+2) \\ \vdots & & \ddots & \vdots \\ h(d+L) & h(d+L-1) & \cdots & h(d+L-T+1) \end{pmatrix} \begin{pmatrix} t(0) \\ t(1) \\ \vdots \\ t(T-1) \end{pmatrix} \\
&= \mathbf{H}_{win}\, \mathbf{t} \qquad\qquad\qquad (2.2)
\end{aligned}
$$

The d here is the delay, and the effective channel outside the window is defined as $\mathbf{c}_{wall}$,

$$
\begin{aligned}
\mathbf{c}_{wall} &= \begin{pmatrix} c(0) \\ \vdots \\ c(d-1) \\ c(d+L+1) \\ \vdots \\ c(L_h+T-1) \end{pmatrix} \\
&= \begin{pmatrix} h(0) & 0 & \cdots & 0 \\ \vdots & \ddots & & \vdots \\ h(d-1) & h(d-2) & \cdots & h(d-T) \\ h(d+L+1) & h(d+L) & \cdots & h(d+L-T+2) \\ \vdots & \ddots & & \vdots \\ 0 & \cdots & 0 & h(L_h-1) \end{pmatrix} \begin{pmatrix} t(0) \\ t(1) \\ \vdots \\ t(T-1) \end{pmatrix} \\
&= \mathbf{H}_{wall}\, \mathbf{t} \qquad\qquad\qquad (2.3)
\end{aligned}
$$

The window and wall of $\mathbf{c}$ are depicted in Fig. 2.1. The expressions of the energy inside and outside the window are

$$
\mathbf{c}_{win}^{\dagger}\mathbf{c}_{win} = \mathbf{t}^{\dagger}\mathbf{H}_{win}^{\dagger}\mathbf{H}_{win}\,\mathbf{t} = \mathbf{t}^{\dagger}\mathbf{A}\,\mathbf{t} \qquad\qquad (2.4)
$$

$$
\mathbf{c}_{wall}^{\dagger}\mathbf{c}_{wall} = \mathbf{t}^{\dagger}\mathbf{H}_{wall}^{\dagger}\mathbf{H}_{wall}\,\mathbf{t} = \mathbf{t}^{\dagger}\mathbf{B}\,\mathbf{t} \qquad\qquad (2.5)
$$

where $\mathbf{A}$, $\mathbf{B}$ are symmetric and positive definite matrices. Optimal shortening could be done by choosing the TEQ $\mathbf{t}$ to maximize the ratio

$$\frac{\mathbf{t}^\dagger \mathbf{A} \mathbf{t}}{\mathbf{t}^\dagger \mathbf{B} \mathbf{t}}, \tag{2.6}$$

subject to $\mathbf{t}^\dagger \mathbf{t} = 1$. Clearly, we could regard such problem as a Rayleigh ratio problem by Cholesky decomposition. Let $\mathbf{B} = \mathbf{C}^\dagger \mathbf{C}$ and $\mathbf{v} = \mathbf{C}\mathbf{t}$, then

$$\frac{\mathbf{t}^\dagger \mathbf{A} \mathbf{t}}{\mathbf{t}^\dagger \mathbf{B} \mathbf{t}} = \frac{\mathbf{t}^\dagger \mathbf{A} \mathbf{t}}{\mathbf{t}^\dagger \mathbf{C}^\dagger \mathbf{C} \mathbf{t}} = \frac{\mathbf{v}^\dagger \mathbf{C}^{-\dagger} \mathbf{A} \mathbf{C}^{-1} \mathbf{v}}{\mathbf{v}^\dagger \mathbf{v}} = \frac{\mathbf{v}^\dagger \mathbf{Q} \mathbf{v}}{\mathbf{v}^\dagger \mathbf{v}}, \tag{2.7}$$

where $\mathbf{Q}$ is appropriately defined. The optimal solution to this problem occurs when the $\mathbf{v}_{max}$ is the eigenvector corresponding to the maximum eigenvalue λ_{max} of $\mathbf{Q}$. In this way, the optimal TEQ could be obtained by

$$\mathbf{t}_{opt} = \mathbf{C}^{-1} \mathbf{v}_{max} \tag{2.8}$$

Therefore, the shortening SIR can be expressed as

$$SIR_{opt} = 10 \log \left(\frac{\mathbf{t}_{opt}^\dagger \mathbf{A} \mathbf{t}_{opt}}{\mathbf{t}_{opt}^\dagger \mathbf{B} \mathbf{t}_{opt}} \right) = 10 \log(\lambda_{max}) \tag{2.9}$$

2.2 MERRY algorithm

The MERRY algorithm is a low complexity, blind channel shortening algorithm. This method takes advantage of the cyclic prefix (CP). If there is no ISI, the samples in the prefix are the same as the last few samples of each block. It exploits the CP redundancy to force the last sample in the equalized CP to be equal to the last sample in the equalized symbol after TEQ. Only one update every DMT samples is needed.

A illustration of the basic concept of the Merry algorithm are given and shown in Fig. 2.2. After the CP is added, the last CP-length samples are identical to the fist CP-length samples in the symbol. Consider that a block of DMT symbol is 8 samples, and the length of the cyclic prefix is 2 samples long. If the channel impulse response has 5 samples, the last sample of cyclic prefix will be $r(2)$ and the last sample of data will be $r(10)$.
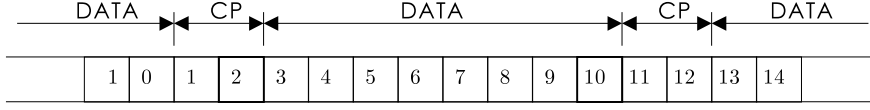
Figure 2.2: Illustration of received $r(n)$ sequence

$$
\begin{aligned}
r(2) &= s(2)h(0) + s(1)h(1) + [s(0)h(2) + s(-1)h(3) + s(-2)h(4)] \\
r(10) &= s(10)h(0) + s(9)h(1) + s(8)h(2) + s(7)h(3) + s(6)h(4) \\
&= s(2)h(0) + s(1)h(1) + [s(8)h(2) + s(7)h(3) + s(6)h(4)]
\end{aligned}
$$

If we add a TEQ $t(n)$ to force the last three sample of channel $h(2) = h(3) = h(4) = 0$, then $r(2) = r(10)$ due to the data repetition in the cyclic prefix $s(2) = s(10)$, $s(1) = s(9)$, and the channel is therefore shortened to order 1 in this case. The cost function that reflects this concept is

$$
J_\triangle = E \left[|y(L + \triangle) - y(L + N + \triangle)|^2 \right] \tag{2.10}
$$

where $\triangle$ is the symbol synchronization parameter. and $y(n)$ denotes the nth sample of receiving DMT symbol at TEQ output. We could make the MERRY update more times per iteration by modifying the cost function into

$$
J_{mod,\triangle} = E \left[\sum_i |y(L + \triangle - i) - y(L + N + \triangle - i)|^2 \right] \tag{2.11}
$$

we introduce another parameter to estimate the instant cost instead of expectation:

$$
J_{inst,\triangle} = \sum_i |y(L + \triangle - i) - y(L + N + \triangle - i)|^2. \tag{2.12}
$$

The gradient could be calculated as,

$$
\frac{\partial J_{inst,\triangle}}{\partial t(l)} = \sum_i [y(L + \triangle - i) - y(L + N + \triangle - i)] [r(L + \triangle - i - l) - r(L + N + \triangle - i - l)] \tag{2.13}
$$

where $r(n)$ denotes the nth sample of receiving DMT symbol with cyclic prefix at TEQ output. We define $\tilde{e}_{i,\triangle} = [y(L + \triangle - i) - y(L + N + \triangle - i)]$ as the

instant error caused by ISI and $\tilde{r}_{i,\triangle} = [r(L + \triangle - i - l) - r(L + N + \triangle - i - l)]$ for convenience. Thus, update of single TEQ parameter could be done by

$$t'(l) = t(l) - \mu \frac{\partial J_{inst,\triangle}}{\partial t(l)} \qquad (2.14)$$

and a normalization is done at the last step of each iteration,

$$\mathbf{t}' = \frac{\mathbf{t}}{\parallel \mathbf{t} \parallel} \qquad (2.15)$$

which avoids the trivial solution of the TEQ.

2.3 The SAM algorithm

SAM is a blind, adaptive channel shortening algorithm. This technique attempts to minimize the sum-squared autocorrelation of the effective channel $\mathbf{c} = \mathbf{h} * \mathbf{w}$ outside a window of the desired length.

The autocorrelation od the effective channel impulse response is defined as

$$R_{cc}(l) = \sum_{k=0}^{L_c} c(k)c(k-l). \qquad (2.16)$$

The parameter L_c denotes the order of combined channel impulse response. For the effective channel response $\mathbf{c}$ to be zero outside a window of size $L + 1$, where L is the CP length. It is necessary for the auto-correlation value $R_{cc}(l)$ to be zero outside the window of length $(2L + 1)$

$$R_{cc}(l) = 0, \forall |l| > L. \qquad (2.17)$$

The cost function of SAM is constructed in attempt to minimize the sum-squared autocorrelation terms

$$J = \sum_{l=L+1}^{L_c} |R_{cc}(l)|^2 \qquad (2.18)$$

and the TEQ optimization problem could be stated as

$$\mathbf{t}^{opt} = arg_{\mathbf{t}} \min_{\mathbf{t}^\dagger \mathbf{t}=1} J. \qquad (2.19)$$

The algorithm requires some assumptions listed as follows:

1. source sequence $s(n)$ is white, zero-mean, and wide sense stationary (WWS).

2. The combined channel order L_c holds the relation $2L_c < M$ for the DMT system, where M is the DFT size.

3. The noise sequence $b(n)$ is zero-mean i.i.d., uncorrelated to the source sequence and has a variance σ_b^2, and the source sequence $s(n)$ is real and has a unit variance.

Consider the auto-correlation function of the sequence $x(n)$,

$$
\begin{aligned}
R_{xx}(l) &= E\left[x(n)x(n-l)\right] \\
&= E\left[(\mathbf{c}^\top \mathbf{s}_n + \mathbf{t}^\top \mathbf{b}_n)(\mathbf{c}^\top \mathbf{s}_{n-l} + \mathbf{t}^\top \mathbf{b}_{n-l})\right] \\
&= \sum_{k=0}^{L_c} c(k)c(k-l) + \sigma_b^2 \sum_{k=0}^{T-1} t(k)t(k-l) \\
&= R_{cc}(l) + \sigma_b^2 R_{tt}(l)
\end{aligned}
\tag{2.20}
$$

The assumption of the input source $s(n)$ is WWS, and is simulated in a ADSL environment. However, the source of ADSL is not WSS since the cyclic prefix is the copy of the last L samples of the output of the DFT matrix. As a result, another assumption $2L_c < M$ is introduced so that there will be no elements correlated with the samples in the cyclic prefix.

Under the noiseless scenario, that is, $\sigma_b^2 = 0$

$$
J = \sum_{l=L+1}^{L_c} |R_{xx}(l)|^2 = \sum_{l=L+1}^{L_c} |R_{cc}(l)|^2
\tag{2.21}
$$

and in the presence of noise, the approximating cost function is

$$
\begin{aligned}
\hat{J} &= \sum_{l=L+1}^{L_c} |R_{xx}(l)|^2 \\
&= \sum_{l=L+1}^{L_c} |R_{cc}(l)|^2 + 2\sigma_b^2 \sum_{l=L+1}^{L_c} R_{cc}(l)R_{tt}(l) + \sigma_b^4 \sum_{l=L+1}^{L_c} |R_{tt}(l)|^2 \\
&\approx \sum_{l=L+1}^{L_c} |R_{cc}(l)|^2
\end{aligned}
\tag{2.22}
$$

16

the TEQ $\mathbf{t}$ have smaller order compare to the length of cyclic prefix, and the noise term σ_b^4 is small then the last term is zero, and the middle term is considered to be neglect.

The adaptive processes are depicted below,

1. calculate the gradients of
$$\frac{\partial J^{inst}(k)}{\partial \mathbf{t}_i}$$

2. update the TEQ coefficients
$$\mathbf{t}_{i+1} = \mathbf{t}_i - \mu \frac{\partial J^{inst}(k)}{\partial \mathbf{t}_i}$$

3. normalize the TEQ coefficients by
$$\mathbf{t}_{i+1} = \frac{\mathbf{t}_{i+1}}{\|\mathbf{t}_{i+1}\|}$$

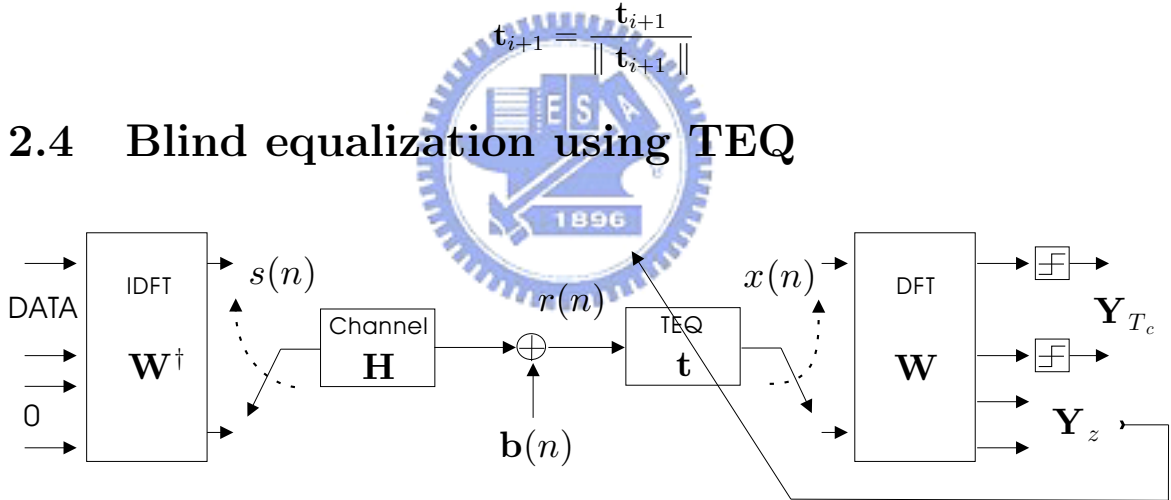## 2.4   Blind equalization using TEQ

Figure 2.3: System model proposed by [14].

In a DMT system, some frequency bins transmit zeros and those frequency bins are called null-carriers. Hence the TEQ is designed to force the energy of the received symbols on the null-carriers to be zero. In [14], since no knowledge on the transmitted data is required, the author propose a blind equalization method.

The cost function is built based on the energy of the demodulation signals of the null-carriers and is expressed as

$$J_z = E\left[\|\mathbf{Y}_z\|^2\right] = E\left[\mathbf{Y}_z^\dagger \mathbf{Y}_z\right] \tag{2.23}$$

17

Because of lacking of guard interval throughout this system the paper used, the zero value input at null tones of the transmitter could not be recovered after passing the DFT processing. With no guard interval added before transmitted, the ISI will occur and exist on the null-carriers. Define

$$
\begin{aligned}
\mathbf{s}_n &= (s(n), s(n-1), \cdots, s(n-M+1))^\top \\
\mathbf{S}_n &= (\mathbf{s}_n, \mathbf{s}_{n-1}, \cdots, \mathbf{s}_{n-M+1})^\top \\
\mathbf{S}^2 &= (\mathbf{S}_n, \mathbf{S}_{n-M+1}) \\
\mathbf{r}_n &= (r(n), r(n-1), \cdots, r(n-M+1))^\top \\
\mathbf{R}_n &= (\mathbf{r}_n, \mathbf{r}_{n-1}, \cdots, \mathbf{r}_{n-M+1})^\top \\
\mathbf{t} &= (t(0), t(1), \cdots, t(M-1))^\top
\end{aligned}
$$

where $s(n)$ denotes the emitted sample and $\mathbf{s}_n$ is a block vector. $r(n)$ is the input of the TEQ and $t(n)$ is the coefficient of the equalizer. The channel is the $2M \times M$ Toeplitz matrix with the first column is given by

$$
\mathbf{h} = (h(0), h(1), \cdots, h(L_c - 1), 0, \cdots, 0)^\top.
$$

and noise is denoted as

$$
\begin{aligned}
\mathbf{b}_n &= (b(n), b(n-1), \cdots, b(n-M+1))^\top \\
\mathcal{B}_n &= (\mathbf{b}_n, \mathbf{b}_{n-1}, \cdots, \mathbf{b}_{n-M+1})^\top
\end{aligned}
$$

where $\mathbf{b}_n$ is a white Gaussian noise of variance σ_b^2. The TEQ output could be expressed as

$$
\mathbf{x} = \mathbf{S}^2 \mathcal{H} \mathbf{t} + \mathcal{B}_n \mathbf{t} \tag{2.24}
$$

After the demodulator, the vector is denoted as

$$
\mathbf{Y} = \mathbf{W}\mathbf{x} = \begin{pmatrix} \mathbf{W}_{T_c} \\ \mathbf{W}_z \end{pmatrix} \mathbf{x} = \begin{pmatrix} \mathbf{Y}_{T_c} \\ \mathbf{Y}_z \end{pmatrix}, \tag{2.25}
$$

where $\mathbf{W}_z$ denotes the rows of the DFT matrix corresponding to the null-carriers and $\mathbf{W}_{T_c}$ represents the rest rows of DFT matrix. The cost function can be rewritten as

$$
J_z = \mathbf{t}^\dagger (\mathbf{P} + \mathbf{Q}) \mathbf{t}, \tag{2.26}
$$

where

$$\mathbf{P} = \mathcal{H}^{\dagger} E \left[\mathbf{S}^{2\dagger} \mathbf{T} \mathbf{S}^2 \right] \mathcal{H} \tag{2.27}$$

$$\mathbf{Q} = E \left[\mathcal{B}^{\dagger} \mathbf{T} \mathcal{B} \right] \tag{2.28}$$

$\mathbf{T}$ is the simplified expression of $\mathbf{W}_z^{\dagger} \mathbf{W}_z$. $\mathbf{t}^{\dagger} \mathbf{t} = 1$ is also included to avoid trivial solution. This optimization could be viewed as a Rayleigh ratio problem, and the optimal $\mathbf{t}$ is the eigenvector associated to the smallest eigenvalue of the matrix $(\mathbf{P} + \mathbf{Q})$.

The adaptive implementation of such cost function could be modified by letting $J_z^{inst} = \mathbf{Y}_z^{\dagger} \mathbf{Y}_z$ to be the instantaneous estimation of the cost function J_z. The adaptive processes are

1. get the output $\mathbf{Y}_z$ and the gradient could be calculated as

$$\frac{\partial J_{z,i}^{inst}}{\partial \mathbf{t}_i^{\star}} = \mathbf{R}_{iM}^{\dagger} \mathbf{W}_z^{\dagger} \mathbf{Y}_z$$

2. update the equalizer

$$\mathbf{t}_{i+1} = \mathbf{t}_i - \mu \frac{\partial J_{z,i}^{inst}}{\partial \mathbf{t}_i^{\star}}$$

3. modify the equalizer into unit norm

$$\mathbf{t}_{i+1} = \frac{\mathbf{t}_{i+1}}{\parallel \mathbf{t}_{i+1} \parallel}$$

With no guard interval there must be interference from the previous symbol. If no noise is considered during the transmission , with the ideal-designed equalization , the values of null tone at the receiver is recovered as zero. It means the TEQ is an inverse of the channel thus the effective channel is an impulse. The author claims that this method leads to shortening to a single spike instead of to a window.

2.5   A frequency-domain SIR maximizing TEQ

This is a semi-blind TEQ design method[16] which maximizes signal-to-interference ratio (SIR) in frequency domain for VDSL systems. The TEQ is designed to exploit the training symbols in VDSL initialization and solved by an eigen approach.

In an VDSL training symbol, some tones are set for pilot tones and others are used for transmitting messages. The pilot tone symbols are determined in a pseudo random manner but the same for all training symbols. In that way, pilot tones contain the information of the channel implicitly. In upstream application, the tones reserved for upstream transmission are called null tones. And in downstream application, the tones reserved for upstream transmission are null tones. Because the noise is zero mean, then after averaged, there is nothing but ISI in null tones.

The objective function is defined as SIR in frequency domain, which is the pilot tones energy over interference in the null tones and message tones,

$$\phi = \frac{\overline{\mathbf{u}}_p^\dagger \overline{\mathbf{u}}_p}{\overline{\mathbf{u}}_m^\dagger \overline{\mathbf{u}}_m + \overline{\mathbf{u}}_n^\dagger \overline{\mathbf{u}}_n},$$

where $\overline{\mathbf{u}}_p$, $\overline{\mathbf{u}}_m$ and $\overline{\mathbf{u}}_n$ represent the output of pilot tones, message tones and null tones, respectively.

The objective function can be formulated as quadratic terms of TEQ coefficients by written in terms of TEQ coefficients.

$$\begin{pmatrix} \overline{\mathbf{u}}_p \\ \overline{\mathbf{u}}_m \\ \overline{\mathbf{u}}_n \end{pmatrix} = \begin{pmatrix} \mathbf{A}_p \\ \mathbf{A}_m \\ \mathbf{A}_n \end{pmatrix} \mathbf{t}$$

The objective function becomes

$$\phi = \frac{\mathbf{t}^\dagger \mathbf{A}_p^\dagger \mathbf{A}_p \mathbf{t}}{\mathbf{t}^\dagger (\mathbf{A}_m^\dagger \mathbf{A}_m + \mathbf{A}_n^\dagger \mathbf{A}_n) \mathbf{t}},$$

and is a generalized Rayleigh quotient.

As $\mathbf{A}_m^\dagger \mathbf{A}_m + \mathbf{A}_n^\dagger \mathbf{A}_n$ is positive definite, it can be written as

$$\mathbf{A}_m^\dagger \mathbf{A}_m + \mathbf{A}_n^\dagger \mathbf{A}_n = \mathbf{B}^{-\dagger} \mathbf{B}^{-1}.$$

Let $\mathbf{v} = \mathbf{B}^{-1} \mathbf{t}$, then $\phi = \frac{\mathbf{v}^\dagger \mathbf{B}^\dagger \mathbf{A}_p^\dagger \mathbf{A}_p \mathbf{B} \mathbf{v}}{\mathbf{v}^\dagger \mathbf{v}}$. ϕ can be maximized by choosing $\mathbf{v}$ to be the eigen vector corresponding to the largest eigen value of $\mathbf{B}^\dagger \mathbf{A}_p^\dagger \mathbf{A}_p \mathbf{B}$. The optimal TEQ is given by $\mathbf{t} = \mathbf{B} \mathbf{v}$.

The TEQ design method can effectively shorten the channel impulse response, and achieve good bit rates with only a small number of training symbols.

Chapter 3

System model

Very-high-bit-rate Digital Subscriber Line (VDSL) system transmits data by means of discrete multitone modulation (DMT) system. In this chapter, DMT system and how VDSL initialization procedure is will be introduced. Besides, to realize the system easily, DMT system is redrawn in matrix representation in this chapter.

3.1 DMT system

DMT is a system which divides the available band into even parallel subchannels or tones. The (de)modulation of DMT is done with an (inverse) fast Fourier transform ((I)FFT). After modulation with an inverse fast Fourier transform (IFFT), a cyclic prefix is added to each block of symbols. Then the reformed symbols are passed though the physical channel and then finally arrive to the receiver to be demodulated.

Because of quite long channel length of very-high-bit-rate digital subscriber line (VDSL), the cyclic prefix should be long enough to be added at transmitting end. That results in less data rate. As a result, a T-tap time-domain equalizer (TEQ) is inserted before demodulation to avoid too long length of cyclic prefix. The goal of TEQ is to shorten the channel impulse response; the DMT system is shown in Fig. 3.1.

In VDSL system, the modulation is done by the inverse fourier transform (IDFT). To generate real time domain transmitted values, the inputs of the IDFT
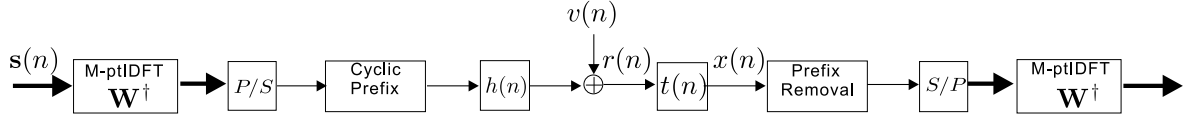
Figure 3.1: DMT system model

matrix are conjugate symmetic. That is, $s_n = s^*_{M-n}$, $n = 1, \cdots, M-1$, where M is the IDFT size. As a result, only $M/2$ QAM symbols can be transmitted each time.

3.2 VDSL initialization

VDSL transceiver shall use Frequency Division Duplexing (FDD) to separate upstream and downstream transmission. The frequency plan shall consist of two upstream bands denoted as 1U, 2U and two downstream bands denoted as 1D, 2D. The bands allocated are shown in Fig. 3.2. The frequency is partitioned according to Table. 3.1.
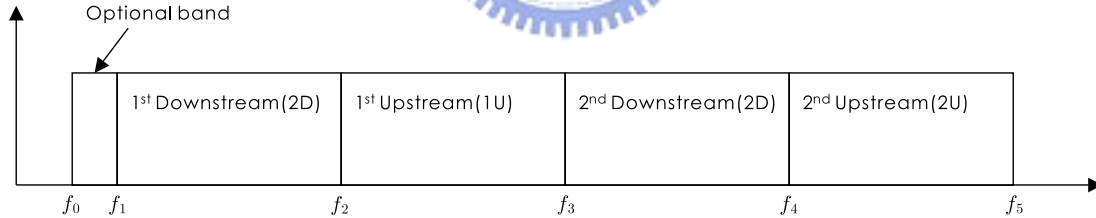

Figure 3.2: VDSL band allocation.

Table 3.1: VDSL band separating frequencies

Separating Frequencies	f_0	f_1	f_2	f_3	f_4	f_5
(MHz)	0.025	0.138	3.75	5.2	8.5	12

The modulation shall use a maximum number of sub-carriers equal to $N_{SC} = 2^{n+8}$, where n can take the values 0, 1, 2, 3, 4. Disjoint subsets of the N_{SC} shell be defined for use in downstream and upstream directions determined by

the frequency plan above (see Fig. 3.2). The frequency spacing, Δf, between the sub-carriers shell be 4.3125KHz.

VDSL uses Frequency Division Duplex to separate all the frequency band to upstream and downstream, respectively. In one of the training stages, only one direction is transmitting while the other direction is silent, not transmitting anything. In this stage, we can assume the signals on the null tones are zeros. Those tones carrying nothing during transmission are taken as null tones and the tones used for transmission are called data tones. As a result, in upstream application, the tones belonging to downstream are the null tones and tones of upstream are the data tones, and vice versa.

Besides, in VDSL training mode, about half of the data tones are set aside for pilot tones. The symbols on the pilot tones are 4-QAM. They are obtained by rotating the constellation point 00 by 0, $\pi/2$, π and $3\pi/2$ in a pseudo-random manner. But the same pilot tones carry the same QAM symbols for all blocks. Even tones and tones that are multiples of 10 plus 9 are reserved for pilot tones. And the rest of the data tones is used for transmitting Special Operation Channel messages (SOC). The information payload of every SOC message shell start with a length of one byte containing a unique code to identify the message and to allow fast and easy recognition of each SOC message. The bit mapping is summarized in Table 3.2 .

Table 3.2: Training symbol bit mapping

Tone index	Constellation point
Even	00
1, 11, 21, $\cdots$,10n+1,$\cdots$	SOC message bits 0,1
3, 13, 23, $\cdots$,10n+3,$\cdots$	SOC message bits 2,3
5, 15, 25, $\cdots$,10n+5,$\cdots$	SOC message bits 4,5
7, 17, 27, $\cdots$,10n+7,$\cdots$	SOC message bits 4,5
9, 19, 29, $\cdots$,10n+9,$\cdots$	00

The selected constellation points (pilot tones) shall be pseudo-randomly rotated by 0, $\pi/2$, π or $3\pi/2$ depending on the value of a 2-bit random number and the sequence is reset each DMT symbol.

3.3 Matrix representation

At the DMT transmitter, the bits are encoded as QAM symbols. In order to have a real transmitted signal, the inputs of the DFT matrix are conjugate symmetry, see Figure 3.1. Then the sequence is added with cyclic prefix (CP) and then transmitted. At the receiving end, the signal passes the TEQ and after that, the prefix will be removed before DFT demodulation. After passing the symbol detector, each tone demodulated could be decoded into bit stream.
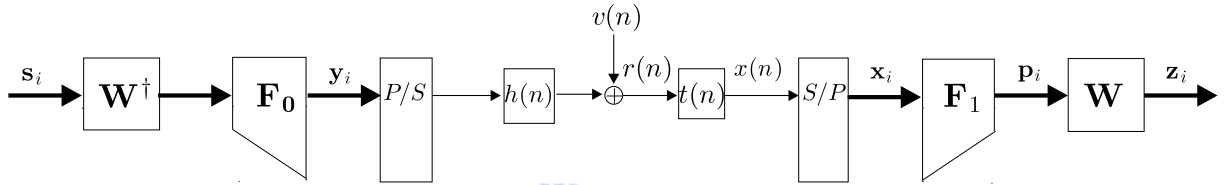

Figure 3.3: The DMT system

To facilitate the analysis, we use a matrix representation and redraw DMT system in Figure 3.1 as Figure 3.3. The matrices $\mathbf{F}_0$ and $\mathbf{F}_1$ in Figure 3.3 are the matrix representation for cyclic prefix insertion and prefix removal. The dimension of $\mathbf{F}_0$ and $\mathbf{F}_1$ are $N \times M$ and $M \times N$ respectively,

$$
\begin{aligned}
\mathbf{F}_0 &= \left(\begin{array}{cc} \mathbf{0} & \mathbf{I}_L \\ & \mathbf{I}_M \end{array} \right), \\
\mathbf{F}_1 &= \left(\begin{array}{cc} \mathbf{0} & \mathbf{I}_M \end{array} \right).
\end{aligned}
\tag{3.1}
$$

L is the length of CP, M is DMT size and $N = L + M$.

From $\mathbf{y}_i$ to $\mathbf{x}_i$, the channel could be represented as an $N \times N$ pseudo-circulant matrix $\mathbf{H}(z)$, given by

$$\mathbf{H}(z) = \begin{pmatrix} h(0) & 0 & \cdots & 0 & z^{-1}h(L_h-1) & \cdots & z^{-1}h(1) \\ h(1) & h(0) & \ddots & \vdots & 0 & \ddots & \vdots \\ \vdots & \vdots & \ddots & 0 & \vdots & \ddots & z^{-1}h(L_h-1) \\ h(L_h-1) & h(L_h-2) & \ddots & h(0) & 0 & \ddots & 0 \\ 0 & h(L_h-1) & \ddots & \ddots & h(0) & \ddots & \vdots \\ \vdots & \ddots & \ddots & \ddots & \ddots & \ddots & 0 \\ 0 & \cdots & 0 & h(L_h-1) & h(L_h-2) & \cdots & h(0) \end{pmatrix}_{N \times N},$$

(3.2)

where L_h is the length of the channel.

As $\mathbf{H}(z)$ is of order one, we can express it as

$$\mathbf{H}(z) = \mathbf{H}_0 + z^{-1}\mathbf{H}_1,$$

where

$$\mathbf{H}_0 = \begin{pmatrix} h(0) & 0 & \cdots & 0 & 0 & \cdots & 0 \\ h(1) & h(0) & \ddots & \vdots & 0 & \ddots & \vdots \\ \vdots & \vdots & \ddots & 0 & \vdots & \ddots & 0 \\ h(L_h-1) & h(L_h-2) & \ddots & h(0) & 0 & \ddots & 0 \\ 0 & h(L_h-1) & \ddots & \ddots & h(0) & \ddots & \vdots \\ \vdots & \ddots & \ddots & \ddots & \ddots & \ddots & 0 \\ 0 & \cdots & 0 & h(L_h-1) & h(L_h-2) & \cdots & h(0) \end{pmatrix}_{N \times N},$$

(3.3)

$$\mathbf{H}_1 = \begin{pmatrix} 0 & 0 & \cdots & 0 & h(L_h-1) & \cdots & h(1) \\ 0 & 0 & \ddots & \vdots & 0 & \ddots & \vdots \\ \vdots & \vdots & \ddots & 0 & \vdots & \ddots & h(L_h-1) \\ 0 & 0 & \ddots & 0 & 0 & \ddots & 0 \\ 0 & 0 & \ddots & \ddots & 0 & \ddots & \vdots \\ \vdots & \ddots & \ddots & \ddots & \ddots & \ddots & 0 \\ 0 & \cdots & 0 & 0 & 0 & \cdots & 0 \end{pmatrix}_{N \times N}.$$

(3.4)

From $\mathbf{y}_i$ to $\mathbf{x}_i$ in Figure 3.3 can be redrawn as in Figure 3.4, where $\mathbf{v}_i$ is $N \times 1$ channel noise vector blocked from $v(n)$. The vector $\mathbf{y}_i$ shown in Figure 3.4 is
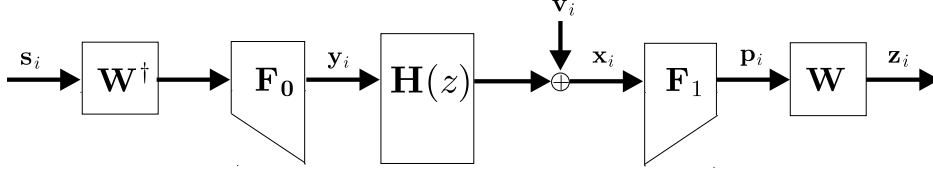
25

Figure 3.4: Matrix representation

given by

$$\mathbf{y}_i = \mathbf{F}_0 \mathbf{W}^\dagger \mathbf{s}_i = \mathbf{F}_0 \mathbf{W}^\dagger \mathbf{P} \begin{pmatrix} \mathbf{s}_{i,p} \\ \mathbf{s}_{i,m} \\ 0 \end{pmatrix}, \tag{3.5}$$

where a permutation matrix P is included so that the input vector can be conveniently expressed as the pilot vector $\mathbf{s}_{i,p}$, followed by message vector $\mathbf{s}_{i,m}$, and null tone vector.

The received vector $\mathbf{x}_i$ can be written as

$$\mathbf{x}_i = \mathbf{H}_0 \mathbf{y}_i + \mathbf{H}_1 \mathbf{y}_{i-1} + \mathbf{v}_i. \tag{3.6}$$

The output vector of the receiver is $\mathbf{z}_i = \mathbf{W} \mathbf{F}_1 \mathbf{x}_i$. For convenience, we permute the outputs into the order of pilot tones and message tones and null tones. Let the receiver output vector after permutation be $\mathbf{u}_i = \mathbf{P}^T \mathbf{z}_i$, then

$$\mathbf{u}_i = \mathbf{P}^T \mathbf{W} \mathbf{F}_1 \mathbf{x}_i = \mathbf{P}^T \mathbf{W} \mathbf{p}_i.$$

Using (3.6) and the expression of $\mathbf{y}_i$ in (3.5), we have

$$\mathbf{p}_i = \mathbf{F}_1 \mathbf{H}_0 \mathbf{F}_0 \mathbf{W}^\dagger \mathbf{P} \begin{pmatrix} \mathbf{s}_p \\ \mathbf{s}_{i,m} \\ 0 \end{pmatrix} + \mathbf{F}_1 \mathbf{H}_1 \mathbf{F}_0 \mathbf{W}^\dagger \mathbf{P} \begin{pmatrix} \mathbf{s}_p \\ \mathbf{s}_{i-1,m} \\ 0 \end{pmatrix} + \mathbf{F}_1 \mathbf{v}_i. \tag{3.7}$$

Notice that $\mathbf{H}_0 + \mathbf{H}_1$ is an N by N circulant matrix and $\mathbf{H}_0 + \mathbf{H}_1 = \mathbf{H}(z)|_{z=1}$, where $\mathbf{H}(z)$ is as defined in (3.3) and (3.4). With $\mathbf{H}_0 + \mathbf{H}_1 = \mathbf{H}(z)|_{z=1}$,

$$\mathbf{u}_i = \mathbf{P}^T \mathbf{W} \mathbf{F}_1 \mathbf{H}_0 \mathbf{F}_0 \mathbf{W}^\dagger \mathbf{P} \begin{pmatrix} \mathbf{s}_p \\ \mathbf{s}_{i,m} \\ 0 \end{pmatrix} + \mathbf{P}^T \mathbf{W} \mathbf{F}_1 \mathbf{H}_1 \mathbf{F}_0 \mathbf{W}^\dagger \mathbf{P} \begin{pmatrix} \mathbf{s}_p \\ \mathbf{s}_{i-1,m} \\ 0 \end{pmatrix} + \mathbf{P}^T \mathbf{W} \mathbf{F}_1 \mathbf{v}_i,$$

where $\mathbf{F}_1 \mathbf{H}_0 \mathbf{F}_0$ can be diagonalized by $\mathbf{W}$ and can be written as

$$\mathbf{F}_1 \mathbf{H}_0 \mathbf{F}_0 = \mathbf{W}^\dagger \boldsymbol{\Lambda} \mathbf{W}.$$

26

Then, $\mathbf{P}^T\mathbf{W}\mathbf{F}_1\mathbf{H}_1\mathbf{F}_0\mathbf{W}^{\dagger}\mathbf{P}\begin{pmatrix} \mathbf{s}_p \\ \mathbf{s}_{i-1,m} \\ 0 \end{pmatrix}$ is the ISI due to other blocks.

Chapter 4

TEQ design

In this chapter, we will exploit properties of VDSL training symbols to design TEQ adaptively. In the frequency-domain SIR maximizing TEQ method in Section 2.5, a fixed number of blocks are first collected before TEQ design is initialed. However, with adaptation, we can train the TEQ coefficients until the adaptation is convergent and stable. This way, we will be free from collecting too many blocks or insufficient number of blocks to design the TEQ. We can stop our adaptation any time when the adaptation is convergent.

When the channel length is shorter than the cyclic prefix added at transmitter, there is no IBI after removing the cyclic prefix at receiver. Under no channel noise, the outputs of the DFT matrix at receiver are the same as the transmitter input symbols scaled by the M-pt DFT of the channel impulse response. In this case, there is nothing but noise on the null tones at receiving end. If the channel length is larger than the cyclic prefix, even though after cyclic prefix removal, there still exists IBI. Therefore, the null tones at receiver contain channel noise and interference from the previous block due to IBI.

Therefore, we propose TEQ designs for VDSL system by minimizing the IBI present on null tones. Assume that the mean of noise and the signals transmitted are nearly zero. If we take the expectation of the DFT output, there is only IBI present on the null tones. If the channel length is shorter than the cyclic prefix, than after taking expectation of the DFT output, the value of the null tones will be zero. The TEQ designs proposed here do not reguire channel impulse

response.

Suppose M_n is the number of null tones, M_p is the number of pilot tones. The numbers of M_d and M_n are determined by the spectral plan. Taking the spectral plan of downstream transmission in Table. 3.1 as an example, $M_p = 962$ and $M_n = 2494$.

In Figure 3.3, suppose the length of TEQ is T, then the TEQ output $x(n)$ can be written as $x(n) = \sum_{l=0}^{T-1} t(l)r(n - l)$. It can also be written in matrix form as follows:

$$
\mathbf{x}_i = \begin{pmatrix} x(iN + \Delta) \\ x(iN + \Delta + 1) \\ \vdots \\ x(iN + \Delta + N - 1) \end{pmatrix}
$$
$$
= \underbrace{\begin{pmatrix} r(iN + \Delta) & r(iN + \Delta - 1) & \cdots & r(iN + \Delta - T + 1) \\ r(iN + \Delta + 1) & r(iN + \Delta) & \cdots & r(iN + \Delta - T + 2) \\ \vdots & \vdots & \ddots & \vdots \\ r(iN + \Delta + N - 1) & r(iN + \Delta + N - 2) & \cdots & r(iN + \Delta - T + N) \end{pmatrix}}_{\mathbf{R}'_i} \underbrace{\begin{pmatrix} t(0) \\ t(1) \\ \vdots \\ t(T - 1) \end{pmatrix}}_{\mathbf{t}},
$$

$$(4.1)$$

where $\mathbf{R}'_i$ is an $N \times T$ convolution matrix and $\mathbf{t}$ is a $T \times 1$ column vector containing TEQ coefficients. $N = L + M$, where L is the length of cyclic prefix and Δ is the synchronization delay.

After removing cyclic prefix, we obtain $\mathbf{p}_i$ expressed as

$$
\mathbf{p}_i = \begin{pmatrix} x(iN + \Delta + L) \\ x(iN + \Delta + L + 1) \\ \vdots \\ x(iN + \Delta + N - 1) \end{pmatrix}.
$$

$$(4.2)$$

Then i-th block of the DFT input vector written in terms of TEQ coefficients

is

$$\mathbf{p}_i = \underbrace{\begin{pmatrix} r(iN+\Delta+L) & r(iN+\Delta+L-1) & \cdots & r_(iN+\Delta+L-T+1) \\ r(iN+\Delta+L+1) & r(iN+\Delta+L) & \cdots & r_(iN+\Delta+L-T+2) \\ \vdots & \vdots & \ddots & \vdots \\ r(iN+\Delta+N-1) & r(iN+\Delta+N-2) & \cdots & r(iN+\Delta-T+N) \end{pmatrix}}_{\mathbf{R}_i} \underbrace{\begin{pmatrix} t(0) \\ t(1) \\ \vdots \\ t(T-1) \end{pmatrix}}_{\mathbf{t}},$$

(4.3)

where $\mathbf{R}_i$ is an $M \times T$ matrix and $\mathbf{p}_i$ is an $M \times 1$ column matrix.

The output vector $\mathbf{z}_i$ of the DFT matrix can be also expressed in terms of TEQ coefficients $\mathbf{t}$ and then permute them to message-tone part, pilot-tone part and null-tone part, respectively. We can use the permutation matrices $\mathbf{P}$ for notational convenience and in this way, the actual pilot tone indices and null tone indices are interleaved.

And then

$$\mathbf{z}_i = \mathbf{W}\mathbf{p}_i,$$

(4.4)

$$\mathbf{P}\mathbf{z}_i = \begin{pmatrix} \mathbf{z}_{i,p} \\ \mathbf{z}_{i,n} \\ \mathbf{z}_{i,m} \end{pmatrix} = \begin{pmatrix} \mathbf{W}_1 \\ \mathbf{W}_2 \\ \mathbf{W}_3 \end{pmatrix} \mathbf{R}_i \mathbf{t},$$

(4.5)

where $\mathbf{W}_1$ is an $M_p \times M$ submatrix which contains the rows corresponding to the pilot tones of the $M \times M$ DFT matrix $\mathbf{W}$, and $\mathbf{W}_2$ is an $M_n \times M$ submatrix which is composed of the rows corresponding to the null tones of DFT matrix $\mathbf{W}$, and $\mathbf{W}_3$ contains the rest rows of DFT matrix $\mathbf{W}$. $\mathbf{z}_{i,p}$ contains the pilot tones and $\mathbf{z}_{i,n}$ contains null tones. $\mathbf{z}_{i,m}$ consists of the non-pilot message tones. After taking expectation, the null tone and pilot tone components can be expressed as,

$$E[\mathbf{z}_{i,p}] = \mathbf{W}_1 E[\mathbf{R}_i]\mathbf{t}$$

and

$$E[\mathbf{z}_{i,n}] = \mathbf{W}_2 E[\mathbf{R}_i]\mathbf{t}.$$

The the pilot tones energy and the null tones energy can be expressed respectively as

$$\mathbf{t}^\dagger \underbrace{E[\mathbf{R}_i]^\dagger \mathbf{W}_1^\dagger \mathbf{W}_1 E[\mathbf{R}_i]}_{\mathbf{A}} \mathbf{t} = \mathbf{t}^\dagger \mathbf{A}\mathbf{t},$$

(4.6)

$$\mathbf{t}^\dagger \underbrace{E[\mathbf{R}_i]^\dagger \mathbf{W}_2^\dagger \mathbf{W}_2 E[\mathbf{R}_i]}_{\mathbf{B}} \mathbf{t} = \mathbf{t}^\dagger \mathbf{B} \mathbf{t}, \tag{4.7}$$

where $\mathbf{A}$ and $\mathbf{B}$ are square matrices of size T. Also, both matrices are positive definite.
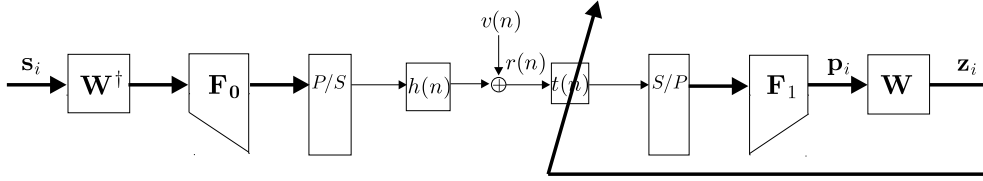
4.1 NM-TEQ (Null tone Minimizing TEQ)

Figure 4.1: Proposed system model

The TEQ proposed here will minimize the null tone energy. If there is no IBI, null tones output should be zero. The cost function of null tone energy can be written as

$$J = E[\mathbf{z}_{in}]^\dagger E[\mathbf{z}_{in}] \tag{4.8}$$

$$= \mathbf{t}^\dagger \underbrace{E[\mathbf{R}_i]^\dagger \mathbf{W}_2^\dagger \mathbf{W}_2 E[\mathbf{R}_i]}_{\mathbf{B}} \mathbf{t} = \mathbf{t}^\dagger \mathbf{B} \mathbf{t}. \tag{4.9}$$

With steepest descent method implemented, the gradient is obtained by

$$\nabla J = \frac{\partial J}{\partial \mathbf{t}} = \frac{\partial \mathbf{t}^\dagger \mathbf{B} \mathbf{t}}{\partial \mathbf{t}} = 2\mathbf{B}\mathbf{t}. \tag{4.10}$$

The iterative update of TEQ is

$$\mathbf{t}_{i+1} = \mathbf{t}_i - 2\mu \mathbf{B} \mathbf{t}_i, \tag{4.11}$$

where μ is the step size which regulates the speed and stability of the adaptation. To avoid a trivial solution, the constraint $\mathbf{t}^\dagger \mathbf{t} = 1$ should be included. That is, normalization of $\mathbf{t}_i$ is performed after each iteration.

The update in (4.11) requires the matrix $\mathbf{B}$, which depends on the channel, not known to the receiver. We can approximate the matrix $\mathbf{B}$ defined in (4.9) by the following average

$$\mathbf{B}_{ave,i} = \overline{\mathbf{R}}\mathbf{W}_2{}^\dagger\mathbf{W}_2\overline{\mathbf{R}}, \tag{4.12}$$

where $\overline{\mathbf{R}} = \frac{1}{i}\sum_{k=1}^{i}\mathbf{R}_k$ and i is the number of iterations. The iterative update with normalization becomes

$$\mathbf{t}_{i+1} = \mathbf{t}_i - 2\mu\mathbf{B}_i\mathbf{t}_i.$$

An instantaneous measure of null tone energy is $\mathbf{t}^\dagger\mathbf{B}_{inst,i}\mathbf{t}$, where

$$\mathbf{B}_{inst,i} = \mathbf{R}_i{}^\dagger\mathbf{W}_2{}^\dagger\mathbf{W}_2\mathbf{R}_i.$$

In this case, then the matrix $\mathbf{R}$ need not be averaged at each iteration. Therefore, the memory required will be reduced and the complexity will also be saved. Those expressions are used throughout the thesis.

4.2 PMNM-TEQ (Pilot tone Maximizing and Null tone Minimizing TEQ)

PMNM_TEQ is the way to maximize the pilot tones energy and minimize the null tones energy. If the noise is zero mean then the null tones consists of ISI only after taking average. And the pilot-tones components imply the information of the channel. The objective function we will minimize is

$$J = \frac{\mathbf{t}^\dagger\mathbf{B}\mathbf{t}}{\mathbf{t}^\dagger\mathbf{A}\mathbf{t}}, \tag{4.13}$$

where $\mathbf{A}$ and $\mathbf{B}$ are defined in (4.6) and (4.7); the expectation can be also approximated by average:

$$\mathbf{A}_{ave,i} = \overline{\mathbf{R}}\mathbf{W}_1{}^\dagger\mathbf{W}_1\overline{\mathbf{R}}$$

and

$$\mathbf{B}_{ave,i} = \overline{\mathbf{R}}\mathbf{W}_2{}^\dagger\mathbf{W}_2\overline{\mathbf{R}}, \tag{4.14}$$

where i is the number of iterations. Similar with NM-TEQ, if we used the instantaneous energy, the complexity will be reduced. For both cases, the objective

functions are in the form of (4.13) In what follows, we will see how to minimize J adaptively. For instantaneous case, the $\mathbf{A}$ and $\mathbf{B}$ matrices are given respectively by, $\mathbf{A}_{inst,i} = \mathbf{R}_i{}^\dagger \mathbf{W}_1{}^\dagger \mathbf{W}_1 \mathbf{R}_i$ and $\mathbf{B}_{inst,i} = \mathbf{R}_i{}^\dagger \mathbf{W}_2{}^\dagger \mathbf{W}_2 \mathbf{R}_i$.

With Cholesky decomposition, $\mathbf{A}$ can be decomposed as $\mathbf{C}^\dagger \mathbf{C}$ and (4.13) can be written as

$$J = \frac{\mathbf{t}^\dagger \mathbf{B} \mathbf{t}}{\mathbf{t}^\dagger \mathbf{C}^\dagger \mathbf{C} \mathbf{t}}. \tag{4.15}$$

Let $\mathbf{v} = \mathbf{C}\mathbf{t}$,

$$J = \frac{\mathbf{v}^\dagger \mathbf{C}^{-\dagger} \mathbf{B} \mathbf{C}^{-1} \mathbf{v}}{\mathbf{v}^\dagger \mathbf{v}} = \frac{\mathbf{v}^\dagger \mathbf{Q} \mathbf{v}}{\mathbf{v}^\dagger \mathbf{v}}, \tag{4.16}$$

where $\mathbf{Q} = \mathbf{C}^{-\dagger} \mathbf{B} \mathbf{C}^{-1}$. Similarly, to avoid trivial solution, the condition $\mathbf{v}^\dagger \mathbf{v} = 1$ should be included. The adaptive iteration is as follows.

$$\mathbf{v}_{i+1} = \mathbf{v}_i - \mu \mathbf{C}^{-\dagger} \mathbf{B}^\dagger \mathbf{C}^{-1} \mathbf{v}_i \tag{4.17}$$

$$\mathbf{v}_{i+1} = \mathbf{v}_{i+1} / \|\mathbf{v}_{i+1}\| \tag{4.18}$$

$$\mathbf{t}_{i+1} = \mathbf{C}^{-1} \mathbf{v}_{i+1}, \tag{4.19}$$

where μ should be chosen properly to guarantee to stability.

Chapter 5

Numerical Simulation

5.1 Environment

The DMT matrix size in the simulation is $M = 8192$ and the length of cyclic prefix is $L = 640$. A 4-QAM modulation is used for the DMT symbol, and downstream bands are used during VDSL initialization. Additive white Gaussian Noise (AWGN) with -140dBm/Hz and Far-end crosstalk (FEXT), near-end crosstalk (NEXT) noise are considered in the simulations.

5.2 Performance measure

The number of bits achieved in i-subchannel is defined as

$$b_i = log_2(1 + \frac{SNR_i}{\Gamma}). \tag{5.1}$$

Γ represents the gap between the channel capacity and the achieved bit rate for a given symbol error. For all the simulations in this thesis, $P_e = 5 \times 10^{-4}$ and $\Gamma = 6.5038$. In VDSL specification, the maximum number of bits on each tone is 15. That is, there are no more than 15 bits loaded on each tone.

5.3 Simulation results

The TEQ used in all simulations has 20 TEQ taps. The measure of the performances is bit rate described in the above section.

There are seven types of VDSL test loops examined, see Table 5.1, and their frequency responses are shown in Figure 5.1.

We use VDSL7 as an example and design TEQ using NM and PMNM methods. The TEQ design using NM method is as shown in Figure 5.2 (a). The frequency response is shown in Figure 5.2 (b). The resulting shortened channel is given in Figure 5.2 (c). Figure 5.2 (d) shows the frequency response of the shortened channel along with the original channel.

The results obtained using PMNM method are given in Figure 5.3(a) to Figure 5.3(d).

These two methods do shorten the original channel. The dotted lines separate the first downstream band (D1) and the second ones (D2) from the null tones.

Table 5.1: VDSL test loop length

Loop	Length (ft.)
VDSL1L	4500
VDSL2L	4500
VDSL3L	4500
VDSL4L	4500
VDSL5	950
VDSL6	3250
VDSL7	4900

The initialization of the TEQ are done as follows: they are minus one at fifth of the TEQ coefficients and one at fourteenth of the TEQ coefficients.
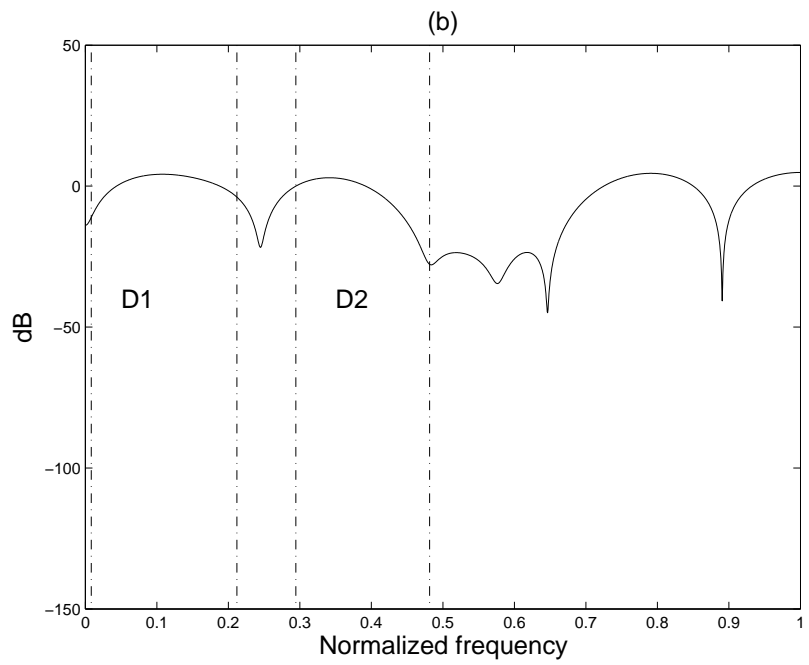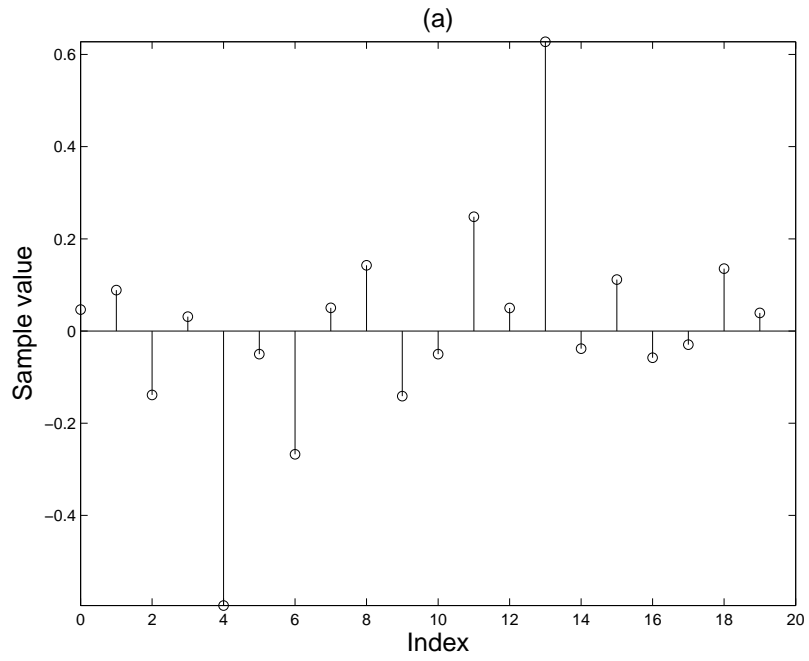
(a)

(b)

(c)

(d)

(e)

(f)
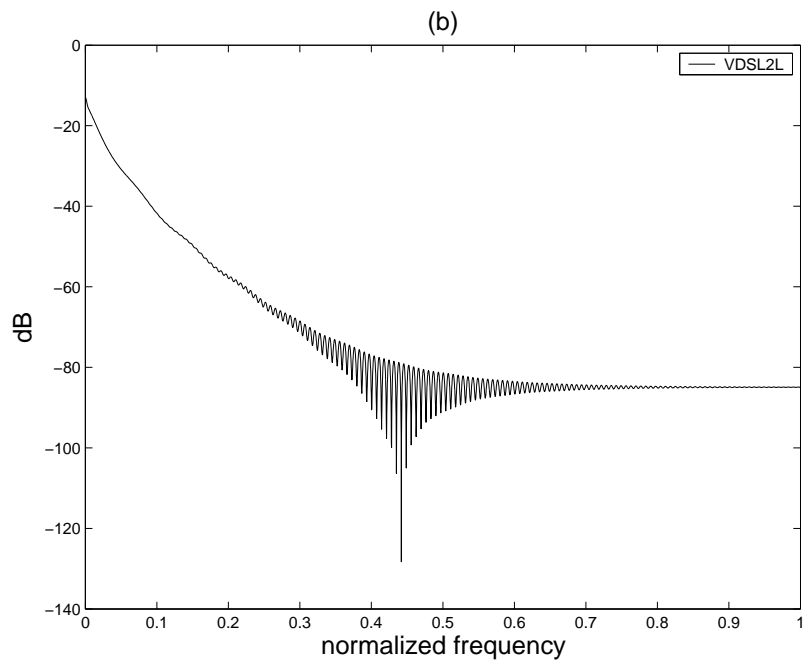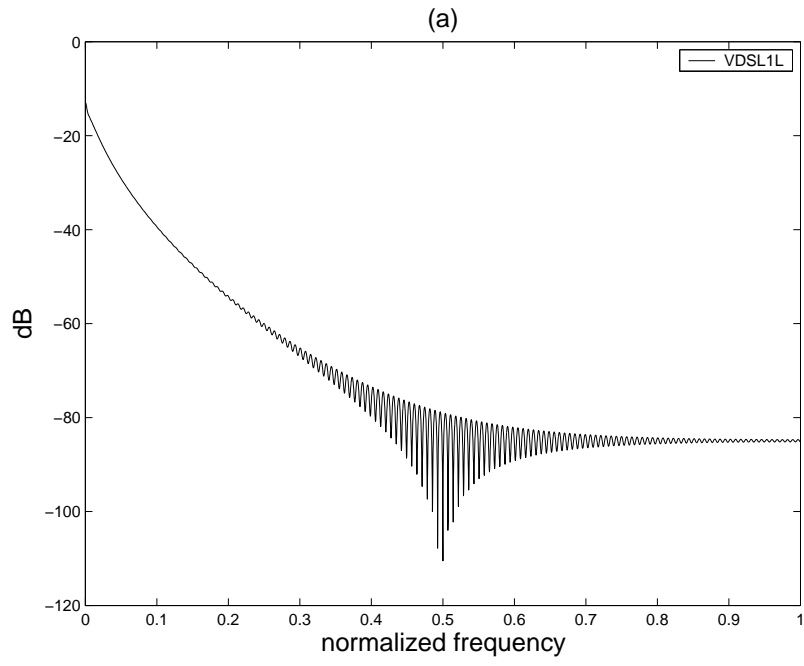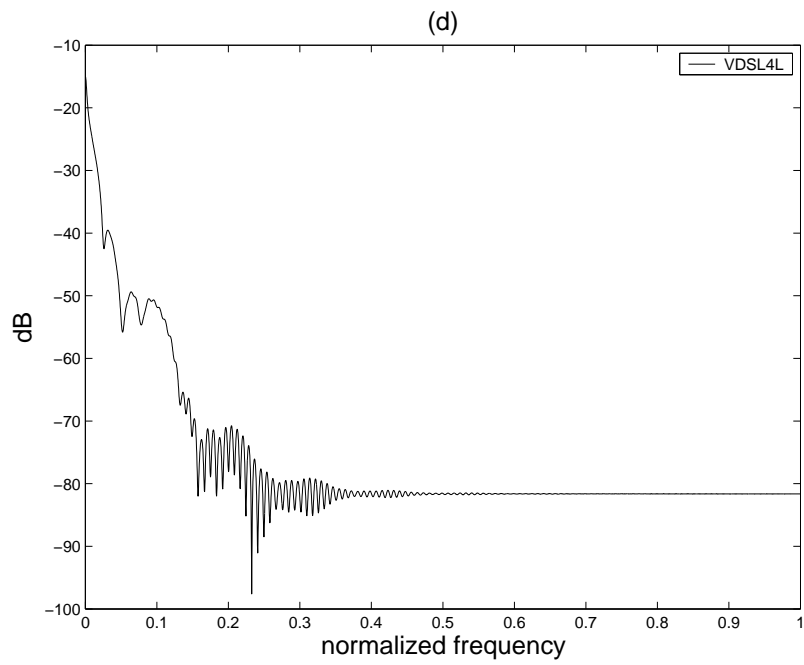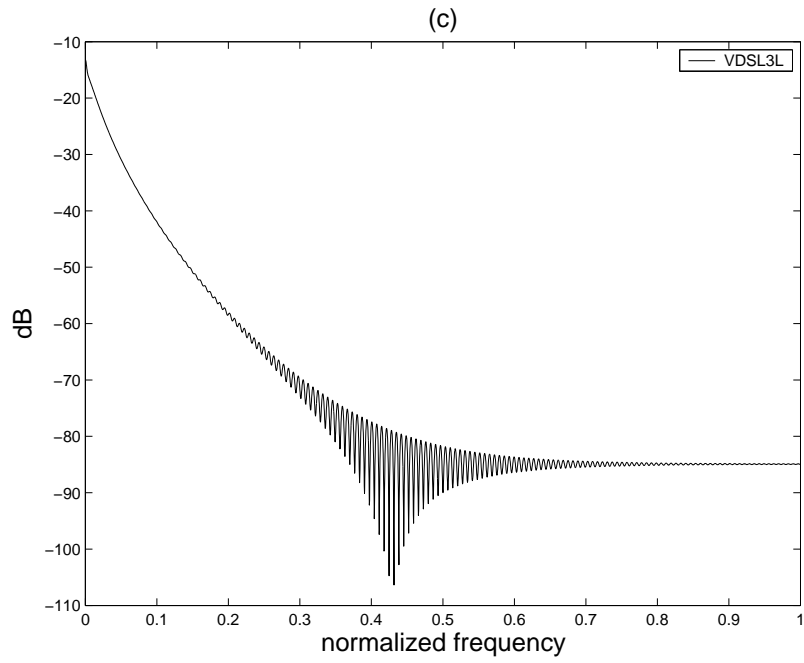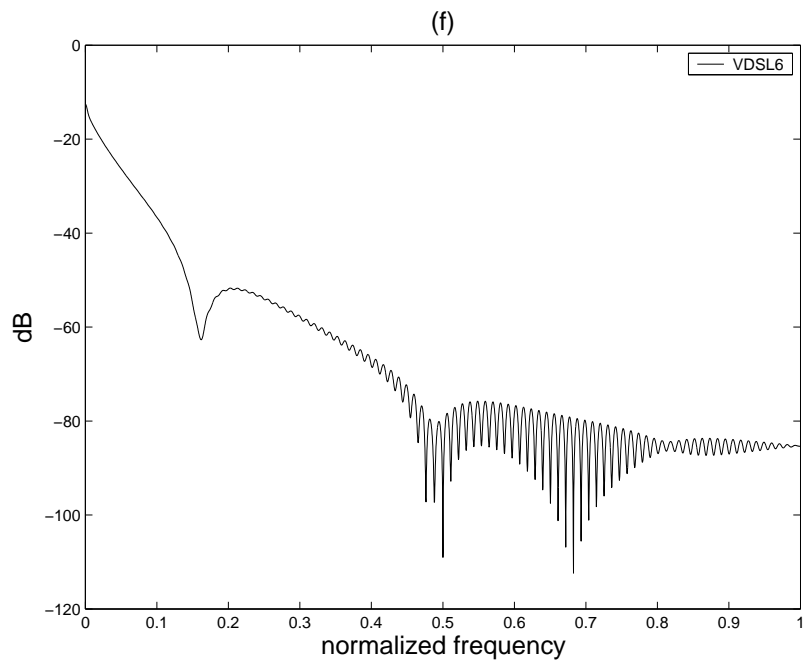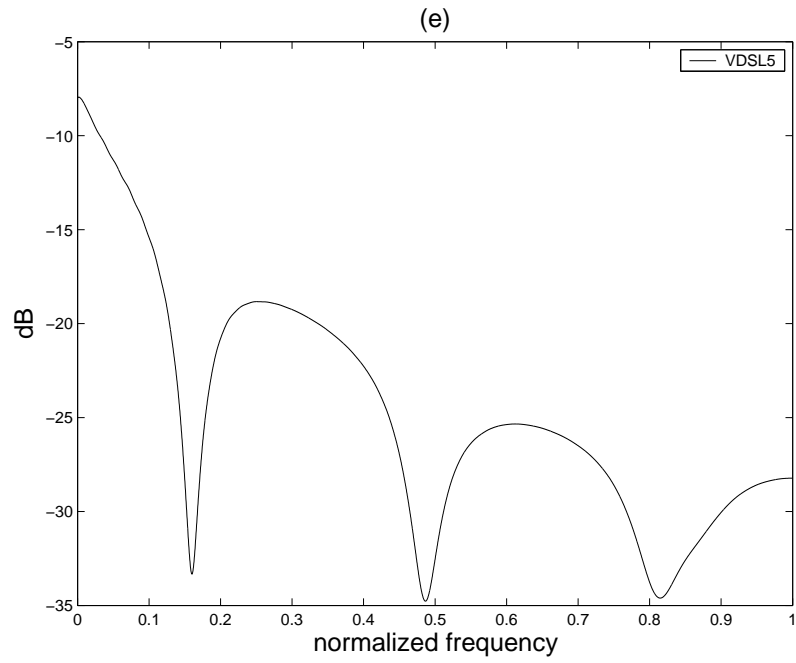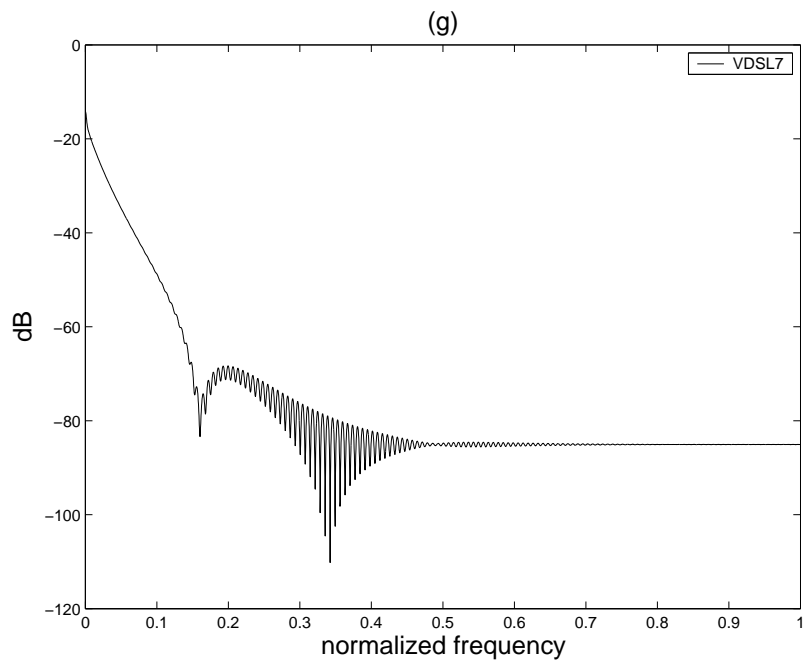
Figure 5.1: Frequency responses of the 7 VDSL loops used in the simulations. (a) VDSL 1L, (b) VDSL 2L, (c) VDSL 3L, (d) VDSL 4L, (e) VDSL 5, (f) VDSL 6, (g) VDSL 7.
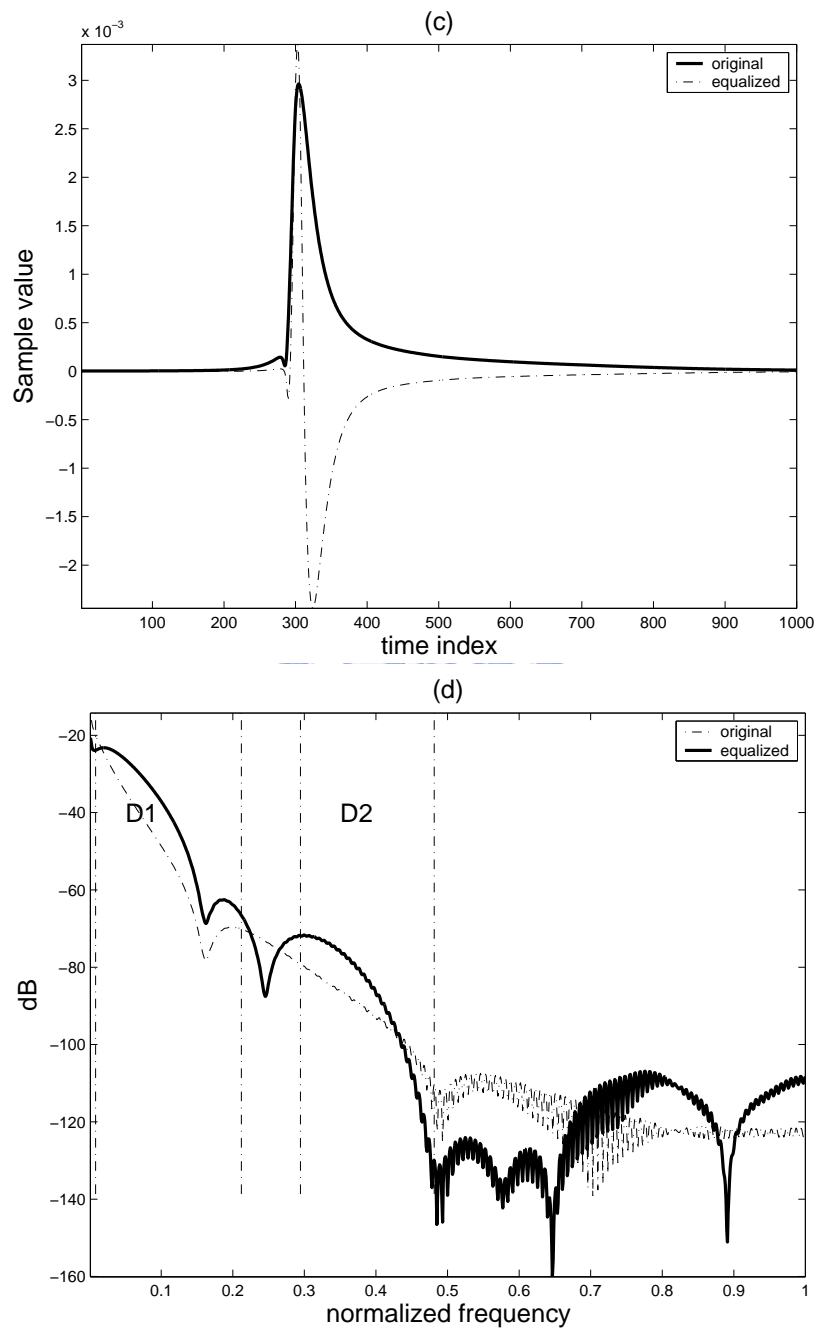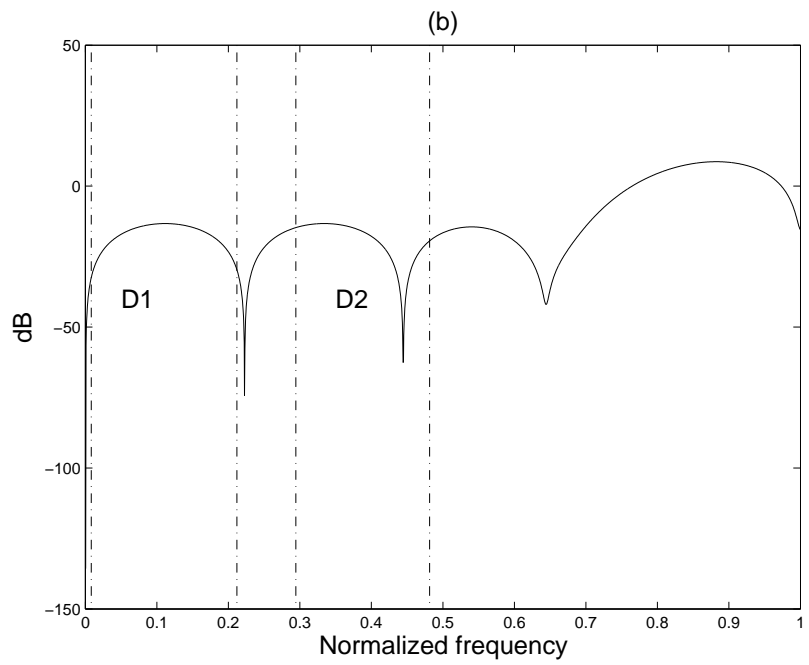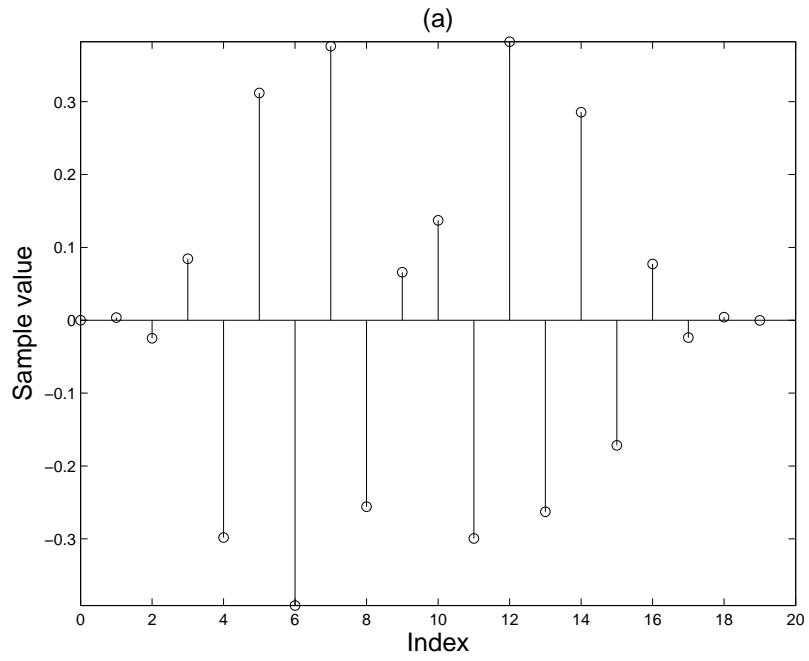
(a)

(b)

Figure 5.2: VDSL7 (a) NM-TEQ impulse response, (b) frequency response of NM-TEQ, (c) the resulting shortened channel, (d) the frequency response of the shortened channel along with the original channel.
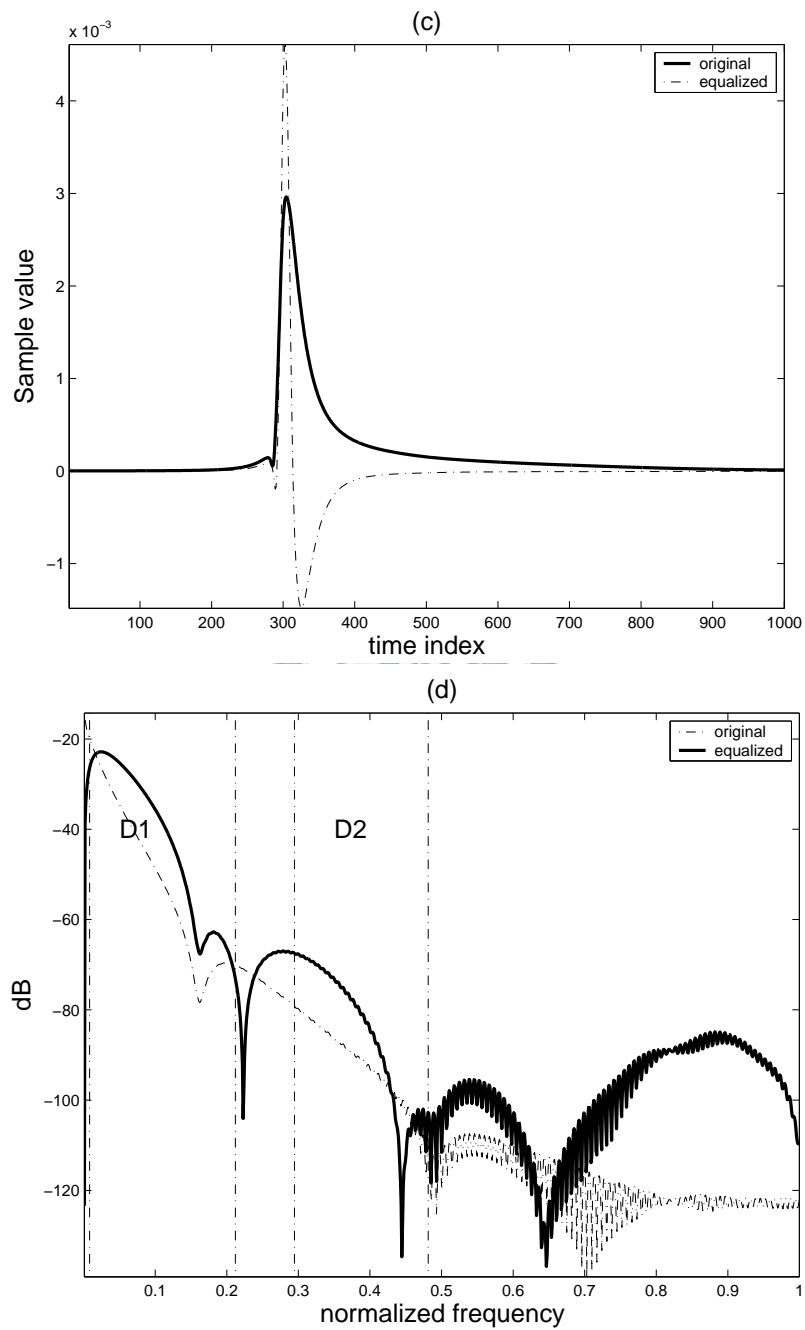
(a)

(b)

Figure 5.3: VDSL7 (a) PMNM-TEQ impulse response, (b) frequency response of PMNM-TEQ, (c) the resulting shortened channel, (d) the frequency response of the shortened channel along with the original channel.

5.3.1 Bit rate comparisons

The comparison of the proposed methods with MSSNR method are shown in Table 5.2. The MSSNR method is discussed in chapter 2. For the NM method, we update the TEQ based on the averaged null tone energy; the **B** in (4.11) is as given in (4.12). For PMNM method, **A** and **B** are as given in (4.14).

Table 5.2: The comparison of NM, PMNM and MSSNR

K bits/sec	NM TEQ	PMNM TEQ	MSSNR
VDSL1L	46,540	44,936	43,212
VDSL2L	41,908	40,848	32,548
VDSL3L	40,900	40,052	37,544
VDSL4L	23,268	22,860	19,332
VDSL5	94,568	92,160	87,916
VDSL6	51,776	49,124	48,028
VDSL7	28,940	28,620	25,492

From Table 5.2, we can observe that all the TEQ methods proposed outperform MSSNR method in bit rates. In our simulations, we have found that the TEQ designed using PMNM method usually have zero in the transmission bands (Figure 5.3 (b)) which results in bit rate loss. As a result, NM-TEQ is usually better than PMNM-TEQ.

We list in Table 5.3 the bit rates with instantaneous energy and average energy of NM-TEQ and PMNM-TEQ when AWGN noise is -140dBm. We can see that there is no significant difference between instantaneous energy and average energy.

5.3.2 Instantaneous v.s average null tone energy

In the NM-TEQ design (section 4.1), we introduced two methods for computing null tone energy, instantaneous null tone energy and average null tone energy. Here we will examine the performance with these two types of methods.

Table 5.4 lists the bit rates with instantaneous null tone energy and average null tone energy under a large AWGN noise, -120dBm and -110dBm. We can see that there is no significant difference between these two methods.

We use VDSL5 as an example and plot the bit rates using these two methods. We can see that the two curves overlap with each other.

Table 5.3: The comparison of NM and PMNM

K bits/sec	NM-TEQ	PMNM-TEQ
VDSL1L	46,896	44,968
VDSL2L	42,044	40,916
VDSL3L	41,072	40,124
VDSL4L	23,336	22,888
VDSL5	94,708	92,156
VDSL6	52,296	49,148
VDSL7	29,004	28,632

Table 5.4: Under different noise environments

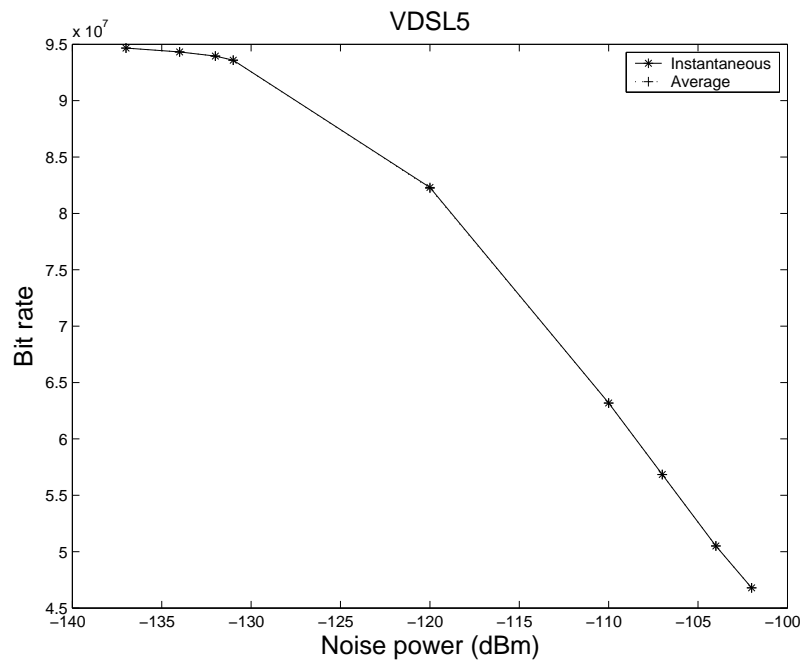| Noise power	-110dBm		-120dBm	
K bits/sec	average	instantaneous	average	instantaneous
VDSL1L	13,060	13,056	22,628	22,636
VDSL2L	11,404	11,408	20,596	20,584
VDSL3L	11,056	11,052	20,028	20,028
VDSL4L	3,480	3,500	8,256	8,256
VDSL5	63,180	63,192	82,236	82,296
VDSL6	13,956	13,940	23,948	23,944
VDSL7	7,704	7,700	13,576	13,572

Figure 5.4: VDSL5 is examined
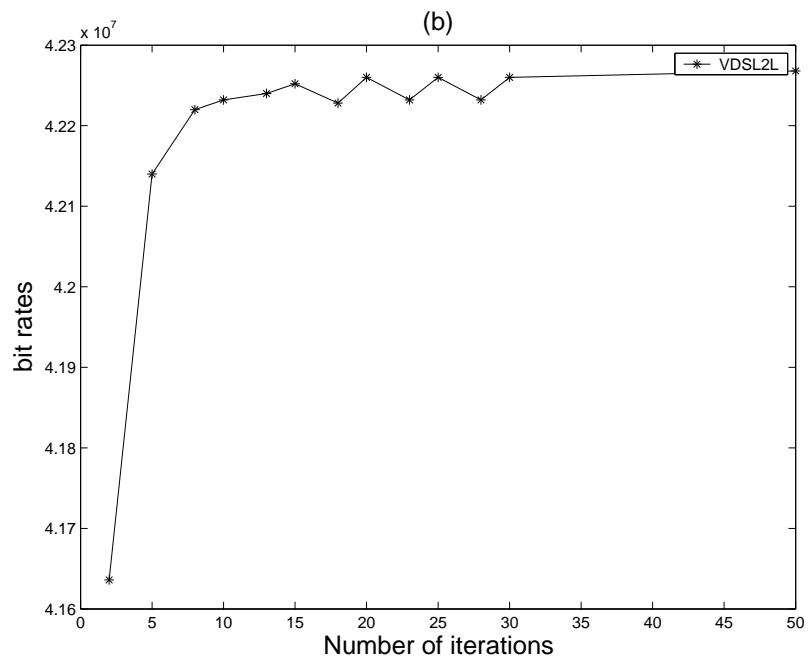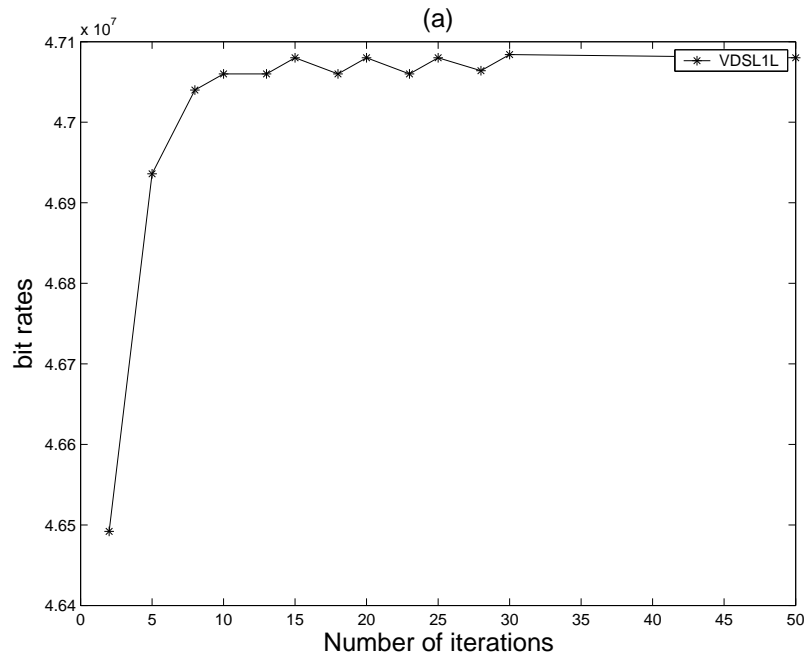
5.3.3 Number of iterations v.s bit rates

In this simulation, we will see how the achievable bit rates of the NM method with instantaneous null tone energy vary with the number of iterations for the seven VDSL loops. From Figure 5.5, it can be observed that the achievable bit rates saturate after 20 iterations for all cases. Using 20 iterations is a good trade off between design efficiency and performance. Therefore, we can stop updating TEQ after 20 iterations. Achievable bit rates for various iterations are given in Table 5.5 and Table 5.6.

Table 5.5: Bit rates with different iterations

K bits/sec	Iter.=2	Iter.=5	Iter.=8	Iter.=10	Iter.=13	Iter.=15
VDSL1L	46,492	46,936	47040	47,060	47,060	47,080
VDSL2L	41,636	42,140	42220	42,232	42,240	42,252
VDSL3L	40,704	41,104	41236	41,236	41,248	41,248
VDSL4L	23,148	23,304	23340	23,344	23,344	23,344
VDSL5	94,700	94,704	94712	94,716	94,720	94,720
VDSL6	51,812	52,376	52452	52,456	52,468	52,476
VDSL7	28,740	29,072	29192	29,220	29,228	29,240

Table 5.6: Bit rates with different iterations

K bits/sec	Iter.=18	Iter.=20	Iter.=23	Iter.=25	Iter.=28	Iter.=30	Iter.=50
VDSL1L	47,060	47,080	47,060	47,080	47,064	47,084	47,080
VDSL2L	42,228	42,260	42,232	42,260	42,232	42,260	42,268
VDSL3L	41,252	41,248	41,252	41,248	41,252	41,256	41,268
VDSL4L	23,348	23,348	23,348	23,348	23,348	23,348	23,352
VDSL5	94,720	94,720	94,720	94,720	94,720	94,720	94,720
VDSL6	52,472	52,484	52,484	52,484	52,488	52,496	52,504
VDSL7	29,236	29,236	29,240	29,236	29,244	29,240	29,244

(a)

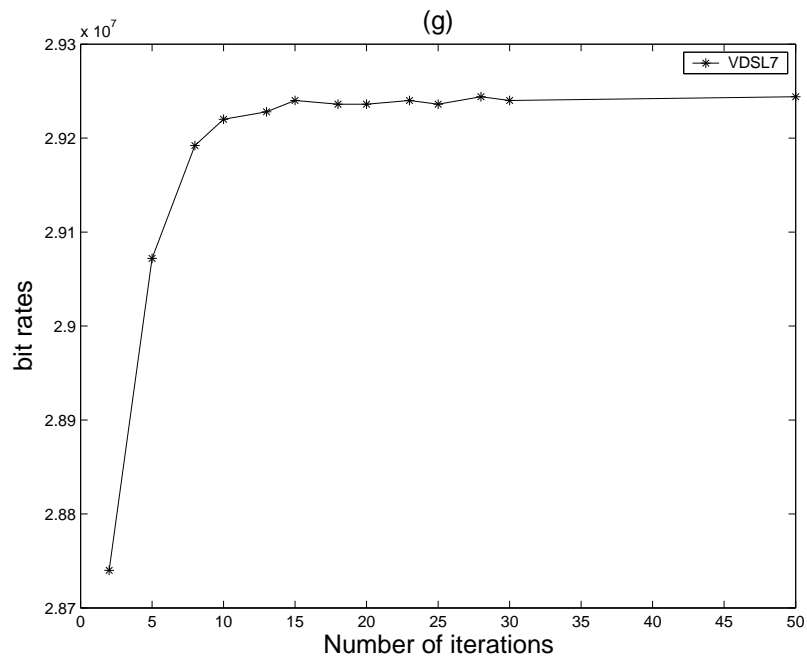(b)

48

(c)

(d)

49

(e)

(f)

50
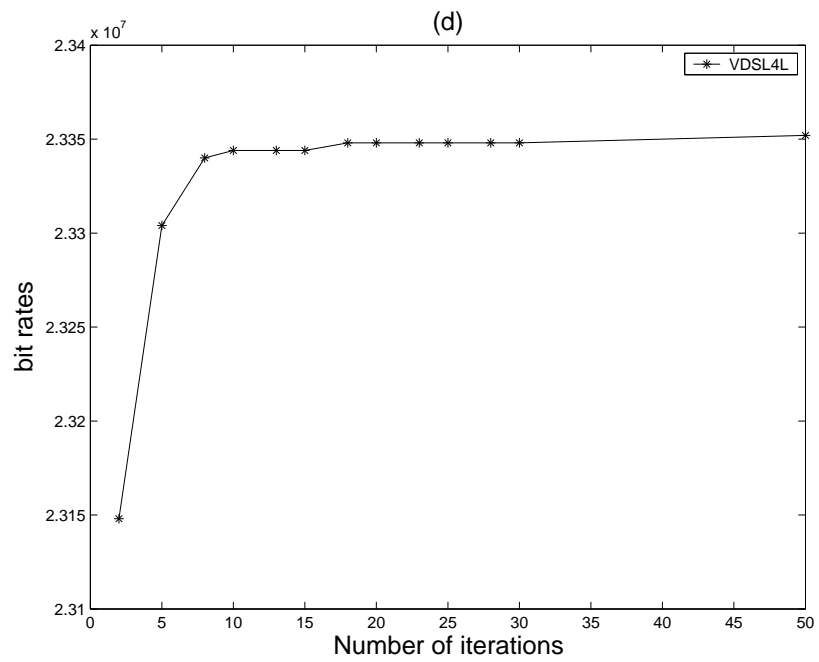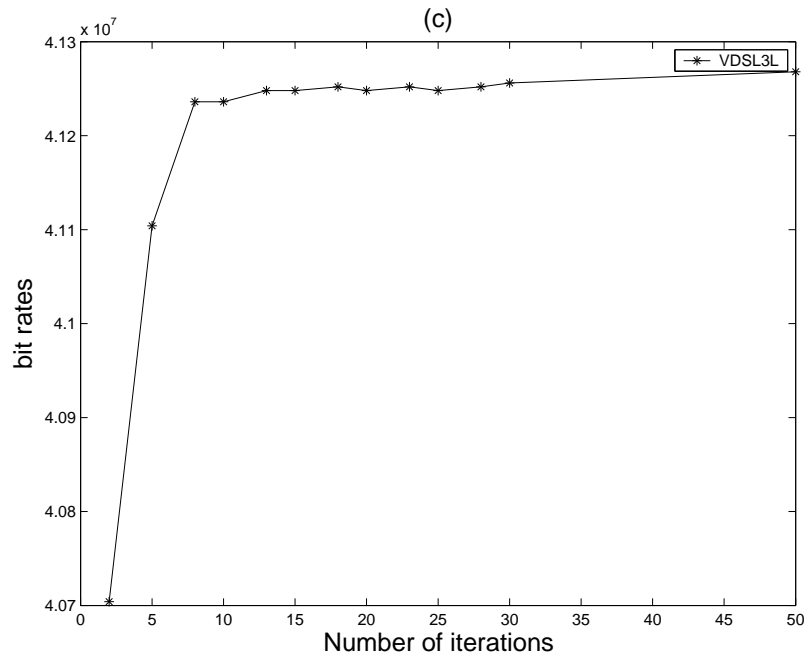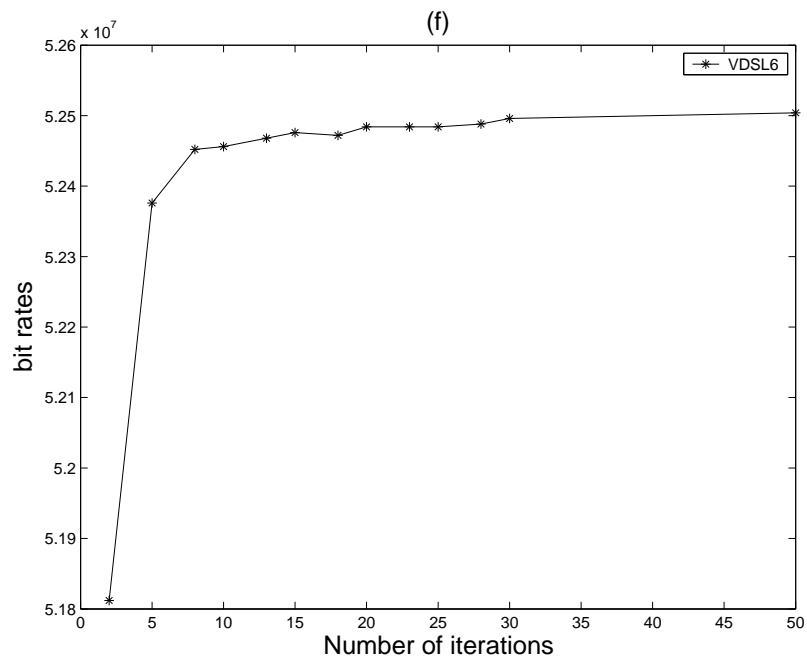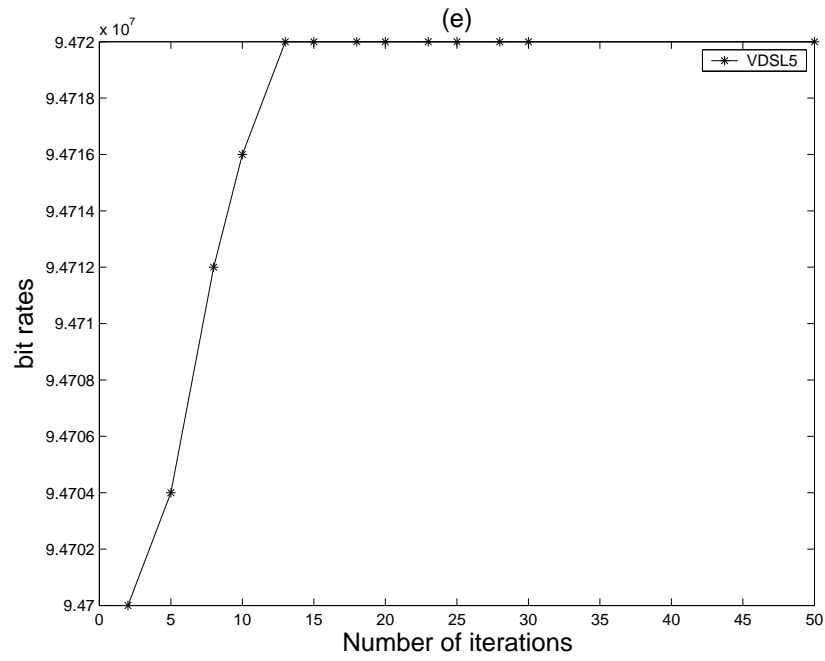
Figure 5.5: Number of iterations v.s bit rates (a) VDSL 1L. (b) VDSL 2L. (c) VDSL 3L. (d) VDSL 4L. (e) VDSL 5. (f) VDSL 6. (g) VDSL 7.
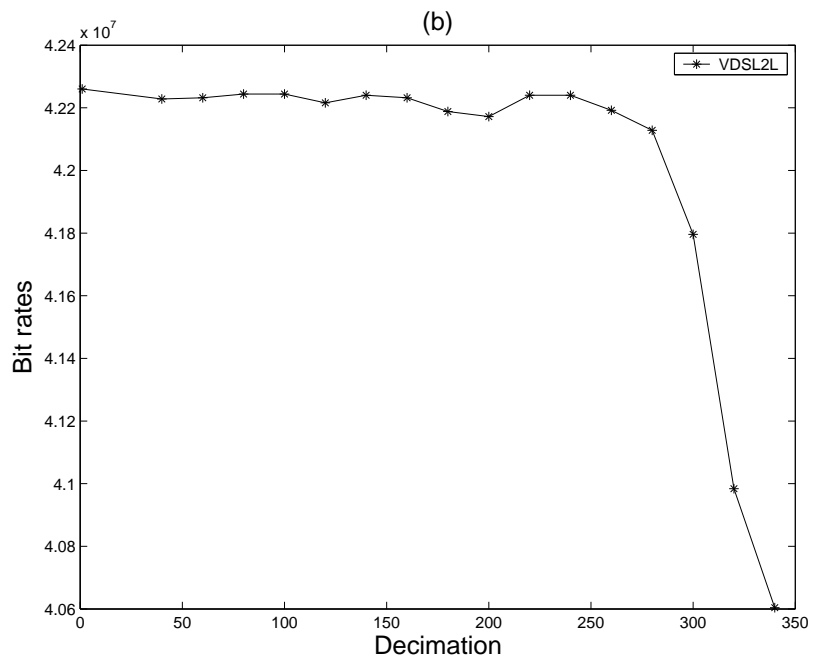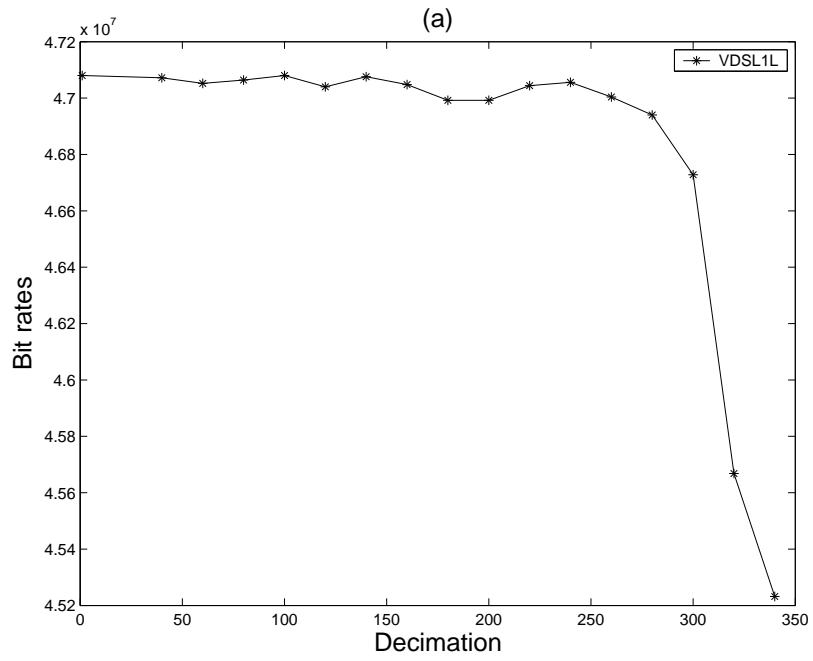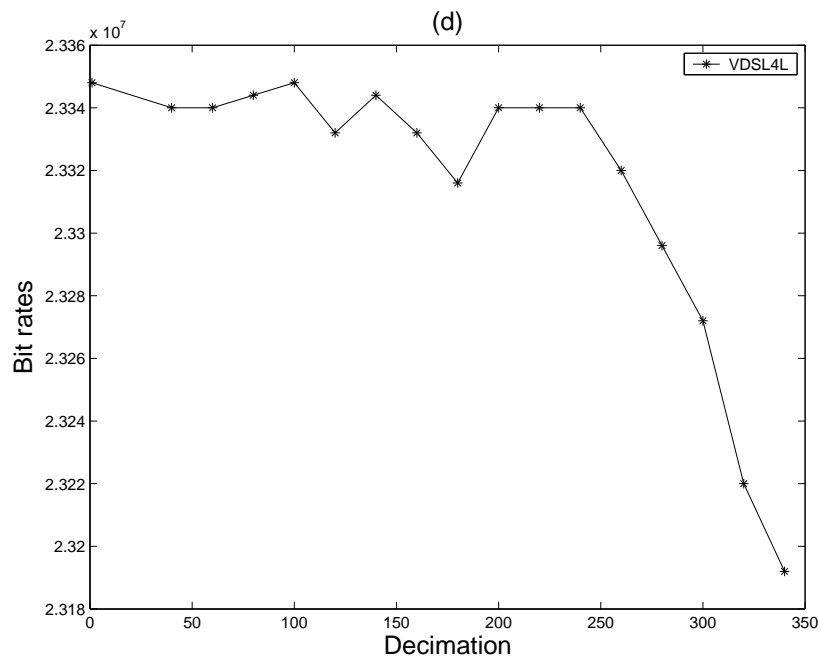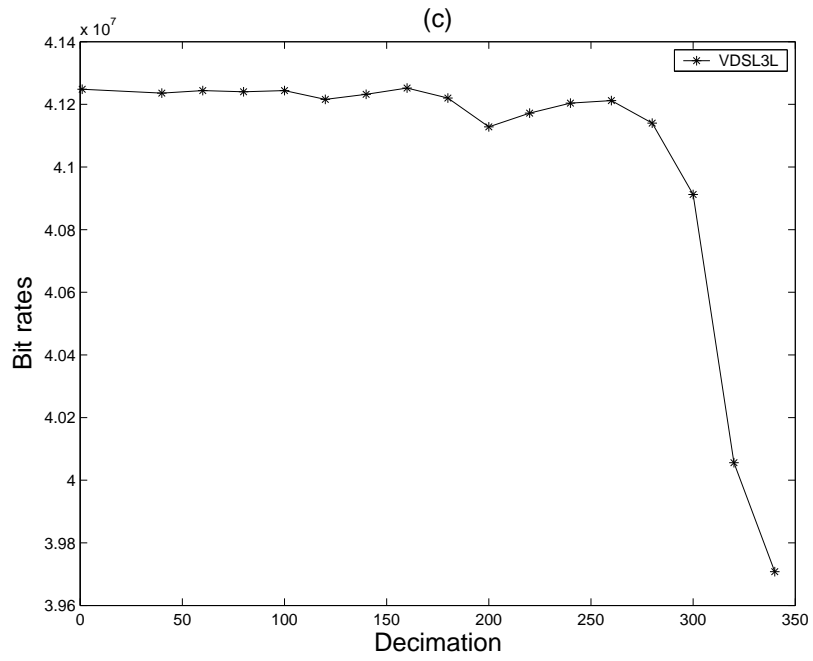
5.3.4 Tone decimation

In section 5.3.1, when we compute the instantaneous null tone energy of NM-TEQ, we use all the null tones. If we use fewer null tones, the computation complexity can be reduced. For this, we can leave out some of the null tones in the formulation of the objective function. For example, we can use only half the null tones; $\mathbf{z}_{in}$ contains only one of every two null tones. The dimensions of $\mathbf{z}_{in}$ will be halved. In this case the new $\mathbf{B}$ contains only the even rows of the original $\mathbf{B}$. More generally, we can choose to decimate the null tones by a number D.

We initialize the TEQ as $t(n) = \delta(n-9)$. The corresponding bit rates with tone decimation are shown in Figure 5.6 for all seven loops (parts of exact bit rates are given in Table 5.7). From the Figure 5.6, we can get similar bit rates with much fewer tones to train the TEQ coefficients, and the complexity will be reduced certainly. From the simulations, we see that the tones can be decimated by 100 without degradation in bit rates.

Table 5.7: Bit rates with different tone decimation

| K bits/sec	Original	$D=40$	$D=60$	$D=80$	$D=100$	$D=120$	$D=140$
VDSL1L	47,080	47,072	47,052	47,064	47,080	47,040	47,076
VDSL2L	42,260	42,228	42,232	42,244	42,244	42,216	42,240
VDSL3L	41,248	41,236	41,244	41,240	41,244	41,216	41,232
VDSL4L	23,348	23,340	23,340	23,344	23,348	23,332	23,344
VDSL5	94,720	94,720	94,720	94,716	94,716	94,720	94,716
VDSL6	52,484	52,480	52,472	52,492	52,480	52,468	52,480
VDSL7	29,236	29,220	29,212	29,212	29,236	29,188	29,208

(a)

(b)

(c)

(d)

54

(e)

(f)
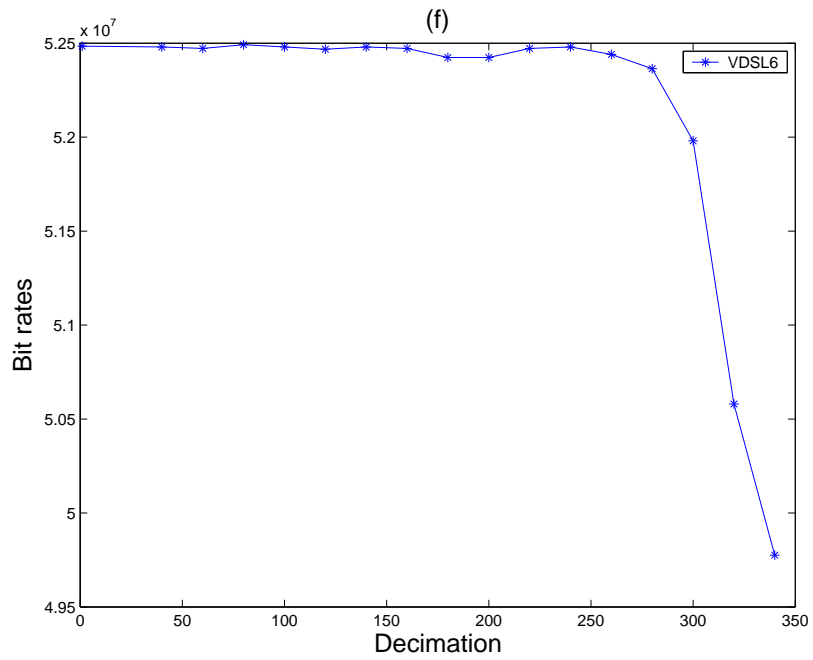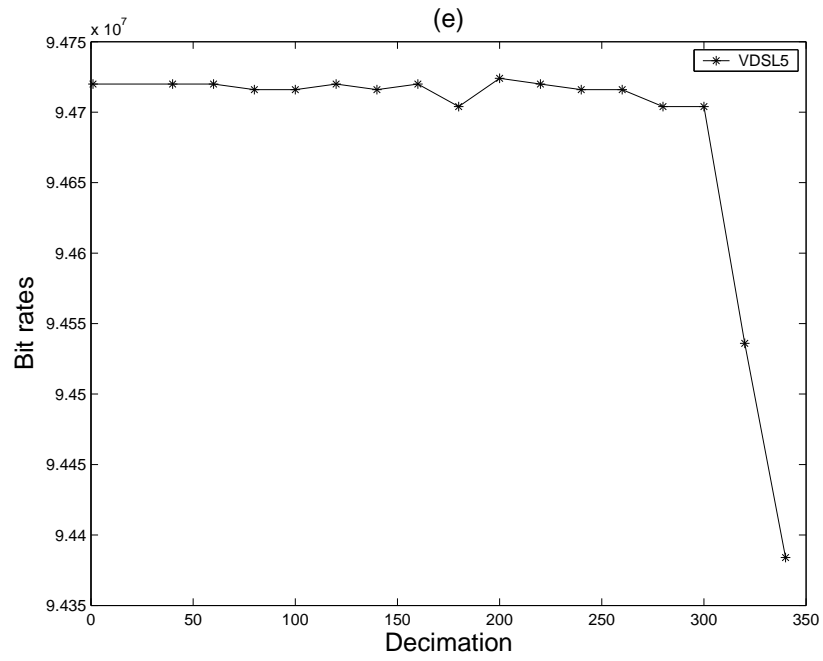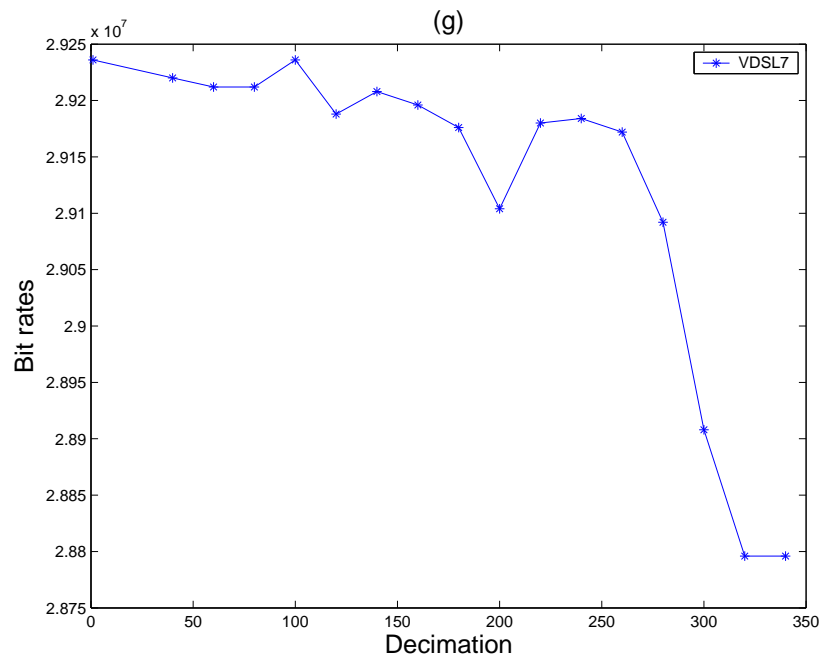
Figure 5.6: Bit rates with tone decimation (a) VDSL 1L. (b) VDSL 2L. (c) VDSL 3L. (d) VDSL 4L. (e) VDSL 5. (f) VDSL 6. (g) VDSL 7.

5.4 Complexity and convergence

In this section, we compare the complexity and convergence of all the adaptive method mentioned earlier, including average and instantaneous cases of NM-TEQ and PMNM-TEQ methods, the case with tone decimation, Merry[12], SAM[13], and the blind[14] methods. The complexity is calculated depending on the number of multipliers, adds, divisions ,and memory used.

Table 5.8: Complexity comparison

complexity/iteration	NM-TEQ	PMNM-TEQ
average	$Mlog_2M + 3MT + 2MT$	$Mlog_2M + T \times M(5/2 + T) + 2MT$
instantaneous	$Mlog_2M + 3MT$	$Mlog_2M + T \times M(5/2 + T)$
decimation D	$M + \frac{3Mlog_2M - 3Mlog_2D}{2D} + (2/D + 1)MT$	$M + \frac{3Mlog_2M - 3Mlog_2D}{2D} + T \times M(T/D + 3/2D + 1)$

In the update equation (4.11) of instantaneous NM-TEQ case, we need to compute $\mathbf{Bt}_i$, which requires $\mathbf{W}_2\mathbf{R}_i$ and multiplying $(\mathbf{W}_2\mathbf{R}_i)^\dagger\mathbf{W}_2\mathbf{R}_i$ and $\mathbf{t}_i$.

1. In (4.9), by using sliding window FFT, the computation of the matrix $\mathbf{WR}$ is $Mlog_2M + T(M + 1)$.

2. multiplying $\mathbf{W}_2\mathbf{R}$ by $\mathbf{t}$ requires $T \times M_u$ multiplications and $(T - 1) \times M_u$ additions.

3. $\mathbf{R}^\dagger\mathbf{W}_2^\dagger\mathbf{W}_2\mathbf{Rt}$ takes $M_u \times T$ multiplications and $(M_u - 1) \times T$ additions.

4. In (4.11), it takes $1 + T$ multiplications and T additions.

For instantaneous PMNM-TEQ case, the complexity is calculated as follows:

1. In (4.17), by applying sliding FFT, the complexity of $\mathbf{WR}$ is $Mlog_2M + T(M + 1)$.

2. With Cholesky decomposition and inverse calculation, it takes $T^3/3$ each.

3. $\mathbf{W}_2\mathbf{RC}^{-1}$ takes $T \times T \times M_u$ multiplications and $(T-1) \times T \times M_u$ additions.

4. $\mathbf{W}_2\mathbf{R}\mathbf{C}^{-1}\mathbf{v}$ takes $T \times M_u$ multiplications and $(T-1) \times M_u$ additions.

5. $\mathbf{C}^{-\dagger}\mathbf{R}^{\dagger}\mathbf{W}_2^{\dagger}\mathbf{W}_2\mathbf{R}\mathbf{C}^{-1}\mathbf{v}$ takes $M_u \times T$ multiplications and $(M_u - 1) \times T$ additions.

6. $\mu\mathbf{C}^{-\dagger}\mathbf{R}^{\dagger}\mathbf{W}_2^{\dagger}\mathbf{W}_2\mathbf{R}\mathbf{C}^{-1}\mathbf{v}$ takes T multiplications and T additions.

7. In (4.19), it takes $T \times T$ multiplications and $(T-1) \times T$ additions.

The complexity of instantaneous NM-TEQ is $Mlog_2M + 4T \times M_u + MT - M_u + 2T + 1$, and that of instantaneous PMNM-TEQ is $Mlog_2M + T((2T+3) \times M_u + M + 2T + 1) + T^3/3 - M_u$, where $M_u \approx M/2$ and the length of TEQ is quite smaller than DFT matrix size. As a result, the complexity of instantaneous NM-TEQ can be approximated by $Mlog_2M + 3MT$ and that of instantaneous PMNM-TEQ can be approximated by $Mlog_2M + T \times M(5/2 + T)$. The average case needs MT multiplications and MT additions more than the instantaneous one.

With tone decimation and by FFT processing, the number of butterflies of each stage can be reduced if decimation is power by 2.

1. if we don't decimate tones, it takes $M/2$ butterflies/stage and there are $log_2M \, stages$ in total. Let M_B=M/2 and $S = log_2M$.

2. when $D = 2$, it takes $M_B \cdot 1$ additions and $M_B \cdot 1/2 \cdot (S - 1)$ butterflies. $M_B \cdot 1$ is the number of additions in the first stage and $M_B \cdot 1/2$ is the number of butterflies per stage in the rest of the stages.

3. when $D = 4$, it takes $M_B \cdot 1 + 1/2 \cdot M_B$ additions and $M_B \cdot 1/4 \cdot (S - 2)$ butterflies, where $M_B \cdot 1 + M_B \cdot 1/2$ is the number of additions in the first stage and second stage, and there are $M_B \cdot 1/4$ butterflies each in the rest of the stages.

4. when $D = 2^n$, it takes $\sum_{k=0}^{n-1} 2^{-k}$ additions and $M_B \cdot 2^{-n} \cdot (S - n)$ butterflies, where $n > 0$, $n \in N$.

Each butterfly takes 1 multiplication and 2 additions. As a result, the complexity with $D = 2^n$ will be

$$\frac{1 - (2^{-1})^n}{1 - 2^{-1}} \cdot M_B + 3 \times M_B \cdot \frac{(S - n)}{2^n}$$

That is, there are

$$\frac{1 - (2^{-1})^n}{1 - 2^{-1}} \cdot \frac{M}{2} + 3 \times \frac{M}{2} \cdot \frac{(log_2 M - n)}{2^n} \approx M + \frac{3M log_2 M - 3nM}{2^{n+1}} = M + \frac{3M log_2 M - 3M log_2 D}{2D} \tag{5.2}$$

.

Taking 8 point FFT for example, when the tones are decimated by 2, the zone of dotted line will be ignored, see Figure 5.7(a). When the tones are decimated by 4, the zone of dotted line will also ignored, see Figure 5.7(b).

Therefore, with tone decimation, the complexity of instantaneous NM-TEQ can be reduced to $M + \frac{3M log_2 M - 3M log_2 D}{2D} + (2/D + 1)MT$ approximately. Similarly, the complexity of instantaneous PMNM-TEQ can be reduced to $M + \frac{3M log_2 M - 3M log_2 D}{2D} + T \times M(T/D + 3/2D + 1)$.

According to Table 5.8, not only the complexity of the average method larger than the instantaneous one, but the average method takes about MT memories more than instantaneous one . Therefore, the instantaneous case is more efficient than the average one. When tone decimation D gets larger, the complexity will be reduced.

Although the complexity of MERRY per iteration is quite low, about $5T$, it takes long iterations to be convergent; for DSL, it takes about 16000 iterations. The complexity of SAM (AR) is $4(T - 1)(L_h + T - 1 - L)$. SAM method needs about 360 iterations to get good performance. The complexity of blind method is $3M^2$. The number of iterations for convergence is not mentioned in the blind method[14]. The proposed two methods, NM-TEQ and PMNM-TEQ, need only a small number of iterations for convergence.
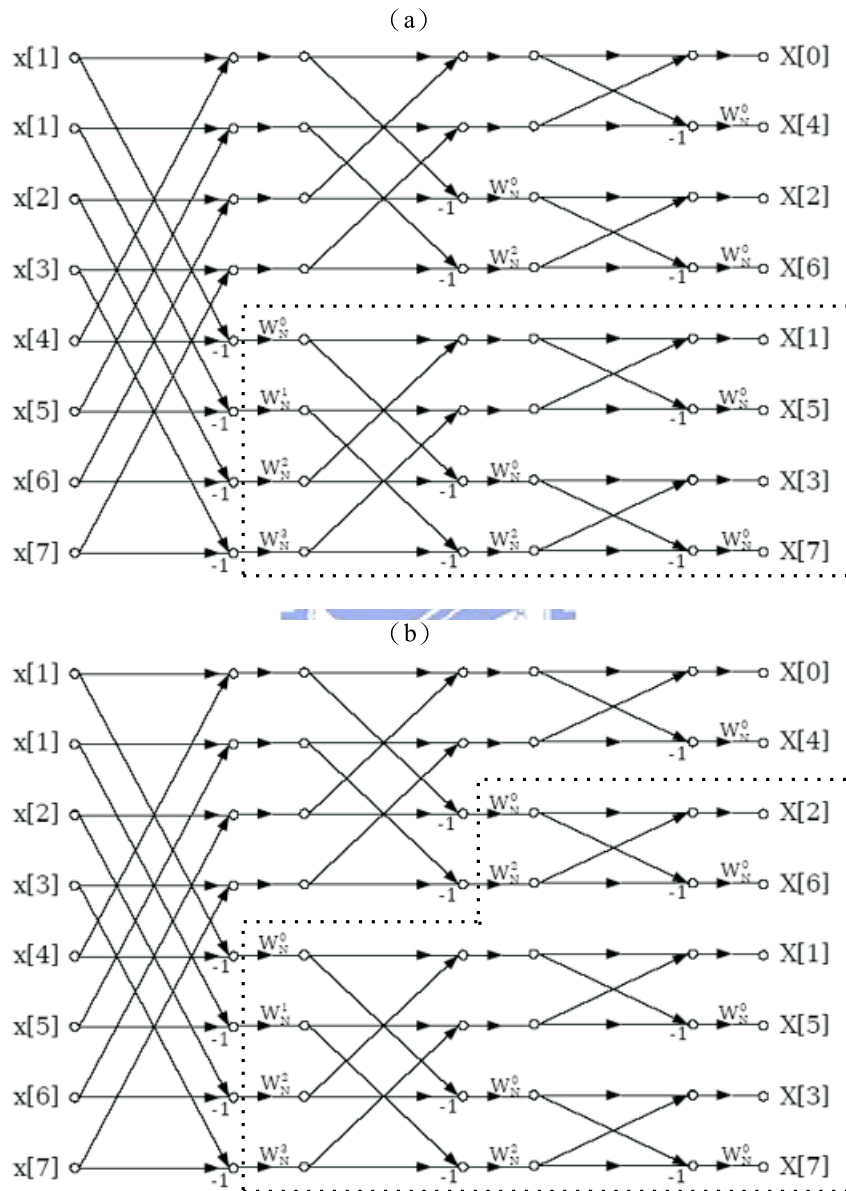
Figure 5.7: FFT (a)$D = 2$ (b)$D = 4$

Chapter 6

Conclusion

In this thesis, two adaptive TEQ designs for VDSL systems are studied. The proposed TEQ designs take advantage of the VDSL training symbols. Using these two methods we can obtain TEQ with satisfying bit rates. The proposed methods achieve bit rates much higher than MSSNR for all test loops. We also examine TEQ performances with objective functions computed using instantaneous energy and average energy. We have found that there is no significant difference between two, even under a large noise environment. Therefore, we can use instantaneous energy in the computation of objective function to save computational cost and memory. Moreover, we have considered tone decimation in the computation of objective function. The simulation results show that we can decimate the tones by as many as 100 without degradation in bit rates.

Bibliography

[1] The European Telecomm. Standards Inst, "*Radio Broadcasting System, Digital Audio Broadcasting(DAV) to Mobile, Portable, and Fixed Receivers,*" *ESTI EN 300 401* 1995-1997.

[2] The European Telecomm. Standards Inst, "*Digital Video Broadcasting(DVB); Framing Structure, Channel Coding and Modulation for Digital Terrestrial Television*" *ESTI EN 300 744 V1.4.1* 2001 Edition.

[3] K. Van Acker, G. Leus, M. Moonen, O. van de Wiel, and T. Pollet, "*Per Tone Equalization for DMT-Based Systems*", *IEEE Trans. on Comm.*, vol. 49, no. 1, pp. 109-119, Jan. 2001.

[4] G. Arslan, B. L. Evans, and S. Kiaei, "*Equalization for Discrete Multitone Receivers To Maximize Bit Rate*", *IEEE Trans. on Signal Processing*, vol. 49, no. 12, pp. 3123-3135, Dec. 2001.

[5] K. Vanbleu, G. Ysebaert, G. Cuypers, M. Moonen, and K. Van Acker, "*Bitrate Maximizing Time-Domain Equalizer Design for DMT-based Systems*", *IEEE Trans. on Comm.*, vol. 52, no. 6, pp. 871-876, June 2004.

[6] K. Vanbleu, G. Ysebaert, G. Cuypers, M. Moonen, and K. Van Acker, "*Bitrate Maximizing Time-Domain Equalizer Design for DMT-based Systems*", *in Proc. IEEE Int. Conf. on Comm.*, May 2003, pp. 2360-2364.

[7] N. Al-Dhahir and J. M. Cioffi, "*Optimum Finite-Length Equalization for Multicarrier Transceivers*", *in Proc. IEEE Global Comm. Conf., San Francisco, CA* , Nov. 1994, pp. 1884-1888.

[8] N. Al-Dhahir and J. M. Cioffi, *"Optimum Finite-Length Equalization for Multicarrier Transceivers"*, *IEEE Trans. on Comm.*, vol. 44, no. 1, pp. 56-64, Jan. 1996.

[9] N. Al-Dhahir and J. Cioffi, *"A Band-optimized Reduced-complexity Equalized Multicarier Transceiver"*, *IEEE Trans. on Comm.*, vol. 45, pp. 948-956, Aug. 1997.

[10] J. S. Chow and J. M. Cioffi, *"A Cost-Effective Maximum Likelihood Receiver for Multicarrier Systems"*, *in Proc. IEEE Int. Conf. on Comm.*, June 1992, vol. 2, pp. 948-952.

[11] R. Schur and J. Speidel, *"An Efficient Equalization Method to Minimize Delay Spread in OFDM/DMT Systems"*, *in Proc. IEEE Int. Conf. on Comm.*, Helsinki, Finland, June 2001, vol. 5, pp.1481-1485.

[12] Martin R.K., Balakrishnan J., Sethares W.A., Johnson C.R. Jr. , *"Blind, adaptive channel shortening for multicarrier systems "* *Signals, Systems and Computers, 2002. Conference Record of the Thirty-Sixth Asilomar Conference* on Nov. 2002 pp.372 - 376 vol.1

[13] Balakrishnan J., Martin R.K., Johnson C.R. Jr., *"Blind, adaptive channel shortening by sum-squared auto-correlation minimization (SAM) "* *Signal Processing, IEEE Tran.* on Dec. 2003 pp.3086 - 3093

[14] M. de Courville, P. Duhamel, P. Madec, and Palicot, *"Blind Equalization of OFDM System Based on the Minimization of a Quadraic Criterion,"* in *Proceedings of the Int. Conf. on Communications,* Dallas, TX, June, 1996.

[15] Melsa P.J.W., Younce R.C., Rohrs C.E., *"Impulse response shortening for discrete multitone transceivers "* *Communications, IEEE Transactions* on ,Dec. 1996 pp.1662-1672.

[16] Lihan Liang, *Desogn of Time Domain Equalizer (TEQ) for VDSL System,* Master thesis, National Chiao Tung University, June 2004.

[17] T1E1/2002-xxx, Trial-Use standard. Draft Trial-Use Standard For Telecommunications Interface Between Networks and Customer Installation Very-high-bit-rate Digital Subscriber Lines(VDSL) interface, "*Alliance for Telecommunications Industry Solutions*"